Politecnico di Milano

SCHOOL OF INDUSTRIAL AND INFORMATION ENGINEERING
Master of Science – Energy Engineering

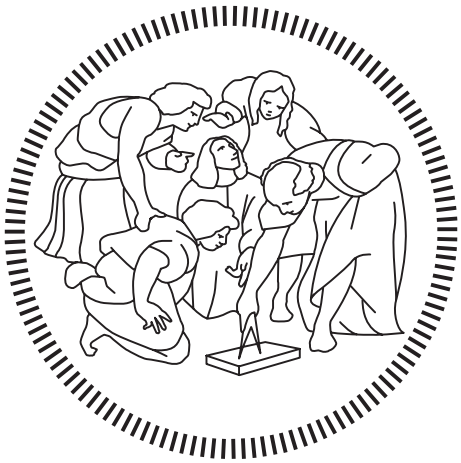

Phtovoltaic Energy production control strategy: Validation of the Reduced Power Point Tracking model

Supervisor
Prof. Roberto Sebastiano FARANDA

Co-Supervisor
Ing. Naga Venkata Kishore Akkala

Candidate
GALPIN Charles-Elie – 879234

Academic Year 2018 – 2019

Acknowledgements

I would like to thank my mom, who has never let me down and gave me the opportunity do fulfill my projects. She has always pushed me to do my best and has never lost faith in my capabilities to reach the point where I am today.

I would like to thank prof. Faranda for offering me the opportunity of working on this thesis. I would like to thank Kishore Akkala for his help and his advices.

I would like to thank Ecole Centrale de Nantes and Politecnico di Milano for giving the opportunity to do a Master in the field I really wanted.

I would like to thank Syed Ali Zaryab and Gianluca Russo, who are always present for the bad and the good moments. There are no words I can say to describe how much I value them and how much I am glad to be their friend.

I would like to thank my team La Pamela Choo, with Angela Dubois and Karla Perdroza, who are always a source of happiness and crazyiness. With Laura Semprini and Alice Previati, what happens is always beyond what is expected.

I would like to thank my Lab 3 team, with Carlos Delgado, Ratomir Dimic, Federico Riva, Arun Shaju, my Halloween's team, with Ali, Fabio Gardella and Giulia Botti, and my Tarot's team. The days and nights spent together are unforgettable and I am glad to have met you all of you guys. I would like to thank also Orkun Gürses with whom the night is always a surprise.

Last but not least, I would like to thank the whole Piacenza students with whom I have shared an amazing adventure.

Sommario

I pannelli fotovoltaici utilizzano il rilevamento del punto di massima potenza. Permette di ottenere la massima potenza disponibile in ogni istante e quindi aumentare l'efficienza del pannello fotovoltaico. In modalità isola o stand alone, potrebbe non essere necessario tenere traccia della potenza massima poiché lo stoccaggio è limitato e il consumo può essere inferiore all'energia utilizzata in un giorno. Collegato alla rete, obbliga la rete a gestire il picco di potenza e questo non è prevedibile. Il rilevamento del punto di alimentazione ridotto limita la potenza non monitorando l'MPPT, ma fornendo la giusta potenza richiesta per ogni istante. Ciò consente al pannello fotovoltaico di diventare programmabile controllando la quantità di energia che deve essere iniettata nel carico. È inoltre necessario che il rilevamento del punto di alimentazione ridotto dia la possibilità di cercare il rilevamento del punto di alimentazione massimo in determinati casi.

Il sistema è composto da un pannello solare, un convertitore DC / DC in cui il carico è direttamente collegato e un sistema di controllo. Il sistema di controllo determina l'alogoritmo del punto di potenza ridotto per determinare il riferimento di tensione e quindi applicato a un controllo della modalità di corrente ibrida, con un integratore proporzionale ad anello esterno per convertire la differenza di tensione nel riferimento di corrente dell'induttore e con l'anello interno usando lo scorrimento controllo della modalità per ottenere il comando del duty cycle che viene quindi inviato al convertitore boost. Un'attenzione speciale è stata posta per i riferimenti perché erano la fonte di errori multipli.

Il compito di questo studio era di determinare il campo di applicazione della tensione per il pannello fotovoltaico. In effetti, poiché due punti possono fingere di fornire la potenza richiesta ma a voltaggio diverso e quindi anche a corrente diversa. I due punti sono rispettivamente denominati lato sinistro e lato destro e si riferiscono al punto di massima potenza. Verranno applicati diversi scenari, il primo la variazione dell'irradiamento e il secondo la variazione della potenza del carico. Qualche teoria è stata vista per valutare la risposta del sistema e verrà quindi verificata con la simulazione. Il risultato ottenuto ha mostrato che il lato sinistro presenta caratteristiche migliori come robustezza e precisione, anche se la rapidità del sistema è ridotta.

Abstract

Photovoltaic panel are using the Maximum Power Point Tracking. It permits to get the maximum power available at each instant and thus increase the efficiency of the PV panel. In island mode or stand alone, it might not be necessary to track the maximum power as the storage is limited and the consumption can be less than the energy used over a day. Connected to the grid, it obliges the network to deal with peak of power and this is not predictable. The Reduced Power Point Tracking limits the power by not tracking the MPPT, but by giving the right power require for each instant. This allows for the photovoltaic panel to become programmable by controlling the amount of power that need to be injected to the load. It is also required that the Reduced Power Point Tracking gives the ability to search the Maximum Power Point Tracking in certain cases.

The system is composed of a solar panel, a DC/DC converter where the load is directly connected, and a control system. The control system results in the Reduced Power Point alogorithm to determine the voltage reference and then applied to an hybrid current mode control, with an external loop proportional integrator to convert the difference of voltage into the inductor current reference and with the internal loop using the sliding mode control to obtain the duty cycle command which is then sent to the boost converter. A special attention has been taken for the references because they were the source of multiple error.

The task of this study was to determine the range of voltage application for the photovoltaic panel. Indeed, since two point can pretend to deliver the power required but at different voltage and thus also to different current. The two points are respectively named left-side and right-side and it is referring to the Maximum Power Point. Different scenarios will be applied, the first one the variation of the irradiance and the second one the variation of the power of the load. Some theory was viewed to evaluate the response of the system and will be then checked with the simulation. The result obtained showed the the left-side presents better characteristic such as robustness and precision, even if the rapidity of the system is reduced.

Table of Contents

List of Figures

List of Tables

Chapter 1
Introduction

The global energy production is composed by 74% from non-renewable sources whereas a mere 26% comes from renewable energy. Furthermore, the energetic demand is constantly increasing implying an ever-growing emission of greenhouse gases and particles that are undoubtedly modifying the global ecosystems. To face these modern challenges, the European Union has focused its attention on the energetic sustainability. For these reasons, the HORIZON 2020 objectives as well as the 2030's where defined in which an increase of the renewable share of 20% by 2020 and of 30% by 2030 are expected [1]. These goals though, were just a part of the overall strategy that the EU set-up to face the issue and try to avoid an ecological cataclysm. Another crucial element, complementary with the increase of renewable share, is the reduction of energy consumption required from every State Member.

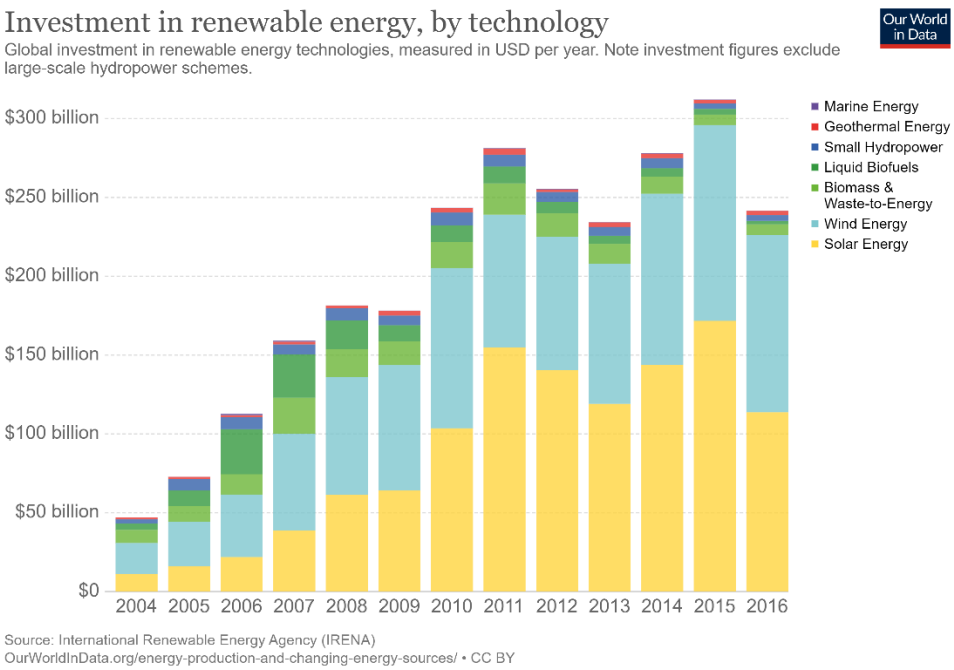

Figure 1.1 Investment in renewable energy, by technology

In the last decades, several renewable energy production technologies were developed in order to keep the pace with the growing interest and awareness of climate change. Figure 1.1 shows that, among the various technologies, the Photovoltaic Technology is doubtless among the most used and developed ones. The technological improvements as well as many financial incentives, allowed this technology to spread and to reduce its costs since from 2009 to 2018, the cost of electricity produced from Photovoltaic Systems (PV systems) decreased by 75% [1].

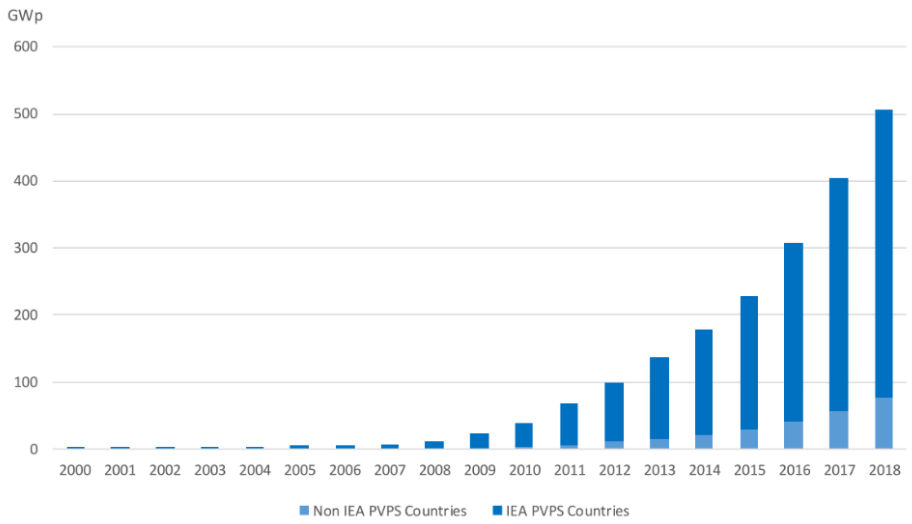

Figure 1.2 Global evolution of PV installation [2]

PV systems are composed by solar cells assembled into a panel to convert the solar power into electric power, two power transfer systems, the first one to control power from the PV panel, the second to change the current from DC to AC, and a control system to control the first power system. The PV systems are very versatile since they can both be installed and compose real power plants commonly called solar farms, but can also be installed on smaller scales and be installed on residential buildings in order to cope with the local loads [2]. This versatility and several politics of incentives [1] enabled this technology to spread at an incredible speed. As we can see in Figure 1.2, the installed Photovoltaic Capacity increased in the last decades with an exponential growth. Today, the EU cumulative capacity installed is estimated to be 114 GW, higher than any other country in the world excepted from China with an overall installed capacity of 176 GW [2], [3].

One of the biggest constraints with Renewable Energy Sources (RES) is their intrinsic non-programmability. Especially when talking about wind and solar energy, the production is strictly related to climatic conditions. Due to this considerable limitation, the connection of these energy sources to the Power Grids have always been limitated in order to avaoid any risk for the safety systems that are currently in place and not effective if a considerable renewable penetration should occur. Even in this domain though, several strategies have

been implemented over the years such as Green Certificates or the development of distributed production and Smart Grids.

It is true though that the versatility that we mentioned earlier, enables these photovoltaic systems to be also independent from any Power or Distributionn Grid and installed in what are called Stand Alone system in which they are coupled with storage systems in order to store the excess production and use it when the system will not be operative, aka at night. This strategy can be very usefull in some conditions (distance from power plants, topography etc) in which the connection to the grid is not possible.

As the technological improvements, the photovoltaic technology reached a deceleration in improvements due to an asymptotum given by the material science involved. Nonetheless, in order to maximize the efficiency, the research have longed study the so-called Maximum Power Point Tracking (MPPT) which permits to the PV panel to produce the maximum power under sunlight variation.
Another idea has been developed recently and can partially solve the problem of the non-programmable RES for the solar PV. The idea is to not look for the Maximum Power Point (MPP), but actually to control the power production with the demand from the needs. This proposed idea implemented in the smart grid can help the stability in case of sunny day, but also for stand-alone network, which for instance the energy demand is very low compared to the available energy that can be produced.

The interest in the MPPT is trivial since the limited efficiency of panels always consisted a crucial limitation to this technology, it is natural that the operators tried to focus on maximizing the power output of their system.

Recently, the researches have pushed forward the study and tried to tackle to issue of the non-programmability of the Photovoltaic Systems. The idea was not to focus only on the Maximum Power Point but to actually adapt the power production according to the needs of the load. This approach, called Reduced Power Point Tracking (RPPT), could be very effective both for stand alone systems as well as the ones implements in conventional or Smart Grids through a more efficient sizing and operational control of the Power Output.

To simulate the behavior of the panels that use this new strategy, several mathematical models were created. This thesis' objective is the study of the mathematical model, used to simulate the behavior of the Photovoltaic Panel using the Reduced Power Point Tracking strategy in stand alone systems. The model will be evaluated in terms of robustness, precision and time of response when a modification on the irradiance or load perturbs the system.

To carry on this study, the methodology used consists in an initial description of the PV cell operation principals and its mathematical modelization as well as a brief overview of the state of the art of the algorithms for the simulation will be performed. Secondly, the control strategies will be analyzed in order to introduce the Reduced Power Point Tracking method. Finally an analysis of the model simulating the RPPT will be performed in order to assess the goodness of the model as well as the determination of the more stable point of functioning.

Chapter 2
Characterization and Modelling of the PV panel

2.1 Solar Cell

A photovoltaic panel is composed of several elements. The most important one is the solar cell. It is generally made from silicon, a material chosen for its structural ability to react to the solar irradiation and convert it into an electrical current, this ability is called the photoelectric effect.

Silicon crystals are semiconductors, meaning that it can act either as an insulator when no energy breaks the bonds between valence electrons, or as a conductor when enough energy is provided for instance by photons. The silicon though cannot generate electricity by itself, it needs to be used into a p-n junction [4], [5].

A p-n junction is composed by two parts, the p-type and the n-type. They are mainly composed by silicon in addition with another element, called dopant. When the silicon is doped with boron atoms, due to its atomic structure which has a lack of electron, it will create excess of holes inside the crystal. When the silicon is doped with phosphorous atoms, it introduces an excess of electrons inside the crystal. This condition is represented in Figure 2.1. On the right side, there is an excess of electrons and on the left side, there is an excess of holes. This combination of holes and free electrons will enable the latters to move and occupy the gaps. Since the negative pole is where the electron starts, the silicon-phosphorous crystal is called the n-type, while the silicon-boron crystal is called the p-type [4], [5].

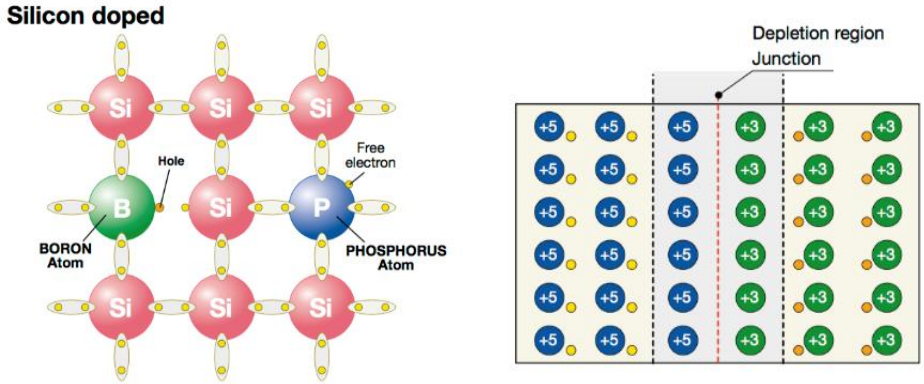

Figure 2.1 Structure of the Silicon crystal doped (left), depletion region (right) [5]

Once we join these two crystals, the free electrons from the n-type will move naturally to the p-type and the holes from the p-type will move to the n-type. This creates an electrical field between the two crystals, and thus forms a potential barrier thanks to the flow of charge. At the equilibrium, the electrons and holes are not able to be mobile and this zone is called the depletion region that can be schematically be seen in the Figure 2.1. This region allows the current to go in only one direction and thus acting as a diode [4], [5]. This similitude will be seen again during the modelization of the photovoltaic cell.

When the solar irradiation reaches the solar cell, the photons excite the electrons and free them as presented in the Figure 2.2. Closing the circuit with a load will force the electrons to move from N to P layer through the load and the holes from the P to N and thus allows a DC current to flow in the circuit. The generated current will directly depend on the amount of photons striking the cell, which can be modelled as a current generator [4], [5].

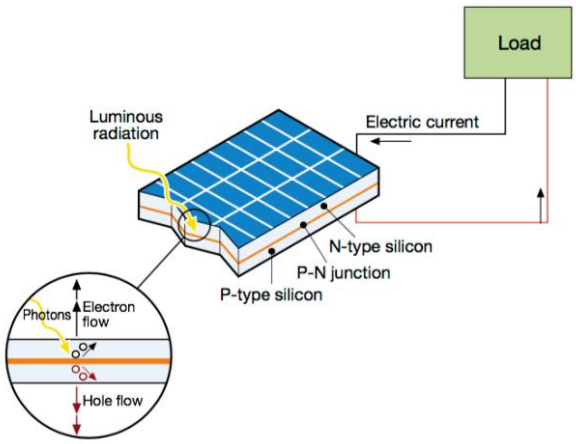

Figure 2.2 Scheme of the circuit with a solar cell and a load [5]

To show the great potential of this technology, it is important to notice that due to losses, the vast majority of the energy carried by the irradiation cannot be converted due to the design of the solar cell [4], [5]:

- 3% Reflection of the solar irradiation from the glass and the electrode
- 23% Photons with high wavelength without enough energy to free the electrons
- 32% Photon with short wavelength with excess energy
- 20% Electric gradient of the cell
- 8.5% Recombination of the free charge carriers

Which leaves about 13% of the solar energy conversion to electric energy.
Figure 2.3 gives an idea of the different reactions that can occur when a photon arrives to the cell like the recombination when the photon enters in the p-layer (3), and the reflection when the photon arrives on the electrodes (4).

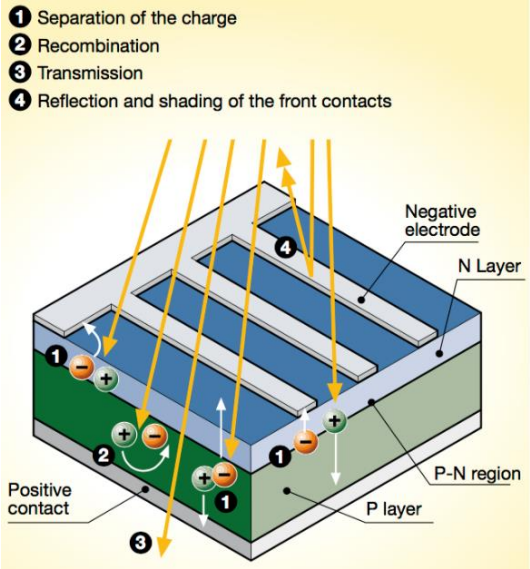

Figure 2.3 Scheme of the solar cell [5]

2.2 Electrical Scheme of the PV panel

2.2.1 Electrical scheme of the cell

Figure 2.4 represents the electrical circuit of the solar cell. It is composed of the photovoltaic cell modelled as current generator, the diode which is necessary to impose the current inside the solar cell, as describe in the previous section. The resistance R_s models the internal resistance to the current flow across the contacts of the different materials. The shunt resistance, R_{sh}, represents the leakage of current of the cell to the earth and strongly depends on the p-n junction and the quality of the crystal.

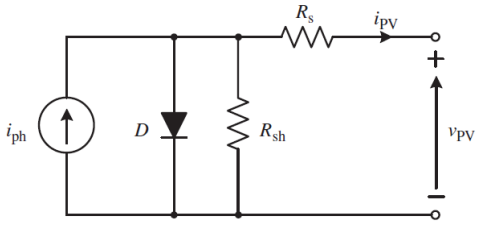

Figure 2.4 Electrical scheme [6]

A cell is defined as a current source with a diode in parallel and the resistance R_{sh}. Then the resistance R_s is connected in series. The current generated by the photovoltaic effect, also called *Photo-Current* I_{ph}. Still, this current is not the one of the panel I_{PV} since it is obtained subtracting the currents absorbed by the diode and the resistance R_{sh}. Finally, V_{PV} represents the voltage of the the PV cell.

2.2.2 The PV panel

A singl photovoltaic cell has a very small power generation capability since it is characterized by a high current but yet a very low voltage. In order to perform and have the possibility to use the photovoltaic panel in normal conditions, it is necessary to connect the cell into specific way so as to get the required power and voltage. Then a specific vocabulary is used so as to understand at which level the cells are interconnected [4]. Usually a module is an assembly of a very small group of cells with a bypass diode so as to limit the losses in case of a default of a cell. On a larger scale, a group of modules can be assembled either in series or parallel to form a panel. Then a group of panels is generally assembled in series so as to reach the required voltage and finally a photovoltaic generator is constituted of a group of arrays connected in parallel in order to get the required power and voltage level. As it comes naturally with the physics, cells connected in parallel are used to increase the current and cells connected in series are used to increase the voltage. Figure 2.5 illustrates the different steps explained.

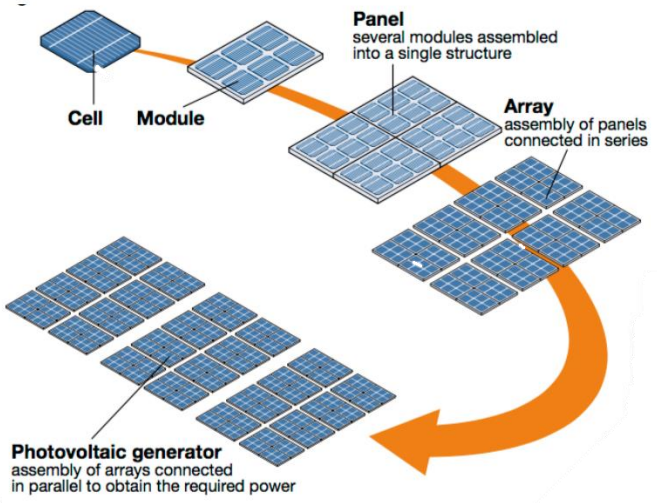

Figure 2.5 Decomposition of the photovoltaic panel [5]

Now that a correct lexic has been defined, we are going to expand the modelization of a single cell to the modelization of many. It is assumed that the cells are similar. Figure 2.6 shows the equivalent circuit with 2 cells in series. The 2 resistances, R_S and R_{sh}, are doubling and the *photo-current* is not affected. Figure 2.7 the equivalent circuit with 2 cells in parallel. In this case, the resistances are divided by 2 and the *photo-current* is multiplied by two. By recurrence to N_s cells in series and N_p cells in parallel, the equivalent circuit is obtained and shown in Figure 2.8. This helps the whole system to reach the required voltage and the required power for a certain design.

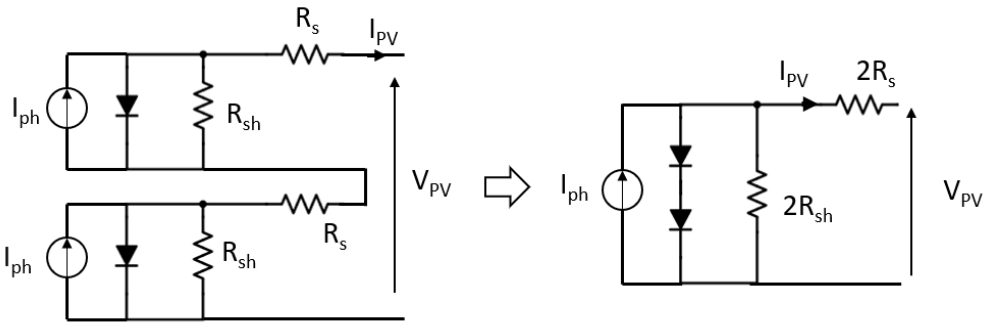

Figure 2.6 Equivalent circuit with 2 cells in series

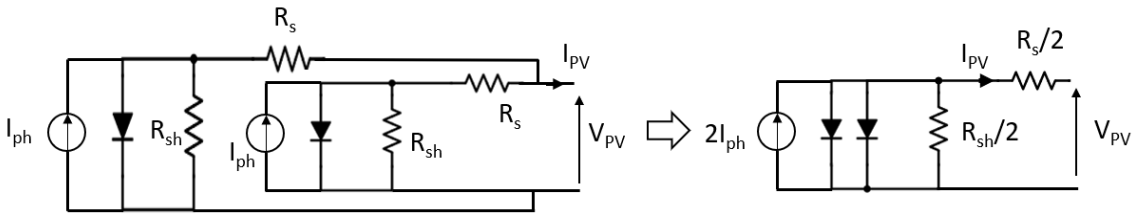

Figure 2.7 Equivalent circuit with 2 cells in parallel

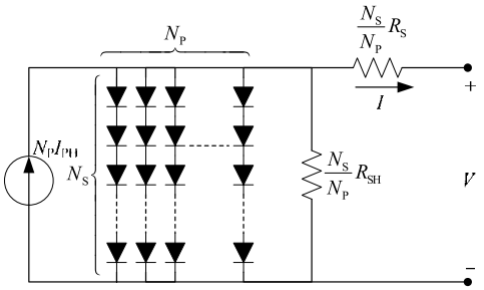

Figure 2.8 General equivalent cricuit PV panel [7]

2.3 Mathematical model

Since the photovoltaic panel is a combination in series and parallel of solar cells, starting from the scheme of the cell, the mathematical model can be obtained easily from Figure 2.8. For further detailed about the equations stated on this section, literature can be found in [7]–[11].

The first equation defined from the Figure 2.8 is the Kirchhoff Current Law using which we obtain the output current of a cell as:

$$I = N_p * I_{ph} - N_p * I_d - I_{sh} \tag{2.1}$$

Where:
$N_p = Number\ of\ Cells\ in\ Parallel$
$I_{ph} = Photo - Current$
$I_d = Diode\ Current$

$I_{sh} = Shunt\ Current$

To have a clear understanding of this equation, the *photo-current, shunt current* and *diode current,* respectively I_{ph}, I_{sh}, I_d, must be calculated.

The *photo-current* is modelized by a current source inside the model. It represents the current produced generated by the photon and is proportional to the solar irradiance. It also depends on the temperature and at ideal conditions, $T = T_{ref}$ and $I_{rr} = I_{r0}$, the *photo-current* is equivalent to the *short-circuit current.* It can be calculated using the following equation:

$$I_{ph} = \left[I_{sc} + K_i \cdot \left(T - T_{ref}\right)\right] \cdot \frac{I_{rr}}{I_{r0}} \tag{2.2}$$

Where
$I_{sc} = Short\ Circuit\ Current\ of\ a\ single\ cell$
$K_i = Reference\ Short\ Circuit\ Current\ of\ a\ cell\ at\ 25°C\ and\ 1000W/m^2$
$T = Temperature$
$T_{ref} = Reference\ Temperature\ (25°C)$
$I_{rr} = Irradiance$
$I_{r0} = Reference\ Irradiance\ (1000W/m^2)$

This formula clearly shows the deep relationship between two key factors in the current generated by a cell. The actual temperature T and the actual irradiance I_{rr}drastically impacts the *photo-current* and the performance of the whole module.

To continue the description of equation 2.1, we must define the *Shunt Current* I_{sh} which represents the current that is dissipated to the earth and is calculated through the Kirchhoff Voltage Law

$$I_{sh} = \frac{V \cdot \frac{N_p}{N_s} + I \cdot R_s}{R_{sh}} \tag{2.3}$$

Where
$V = Total\ Voltage\ of\ the\ Photovoltaic\ Panel$
$I = Total\ Current\ of\ the\ photovoltaic\ panel$
$R_s = Internal\ Resistance\ of\ a\ cell$
$R_{sh} = Shunt\ Resistance\ of\ a\ cell$

Finally, the *diode current* I_d must be estimated to conclude the description of the variables involved in equation 2.1 used to calculate the current of a photovoltaic module. It models the p-n junction due to the similitude of the characteristics as a semi-conductor.
I_d can be calculated by:

$$I_d = I_D \cdot \left[exp\left(\frac{\frac{V}{N_s} + I \cdot \frac{R_s}{N_p}}{nV_T} \right) - 1 \right] \quad (2.4)$$

Where
$I_D = Saturation\ Current$
$V = Total\ Voltage\ of\ the\ photovoltaic\ panel$
$I = Total\ Current\ of\ the\ photovoltaic\ panel$
$R_s = Internal\ Resistance\ of\ a\ cell$
$n = Ideal\ factor\ of\ the\ diode$
$V_T = Thermal\ Voltage$

This formula, describing the current consumed by the diode highlights the relationship between the voltage of the photovoltaic panel and its current. The equation also shows the non-linear behavior of the the photovoltaic panel since the exponential function is involved inside the equation 2.4. When a negative voltage is applied to the diode, which mean that the current is sent through the n-side to the p-side inside the p-n junction. A small current is thus generated and noted *Saturation current.*

Since the diode models a part of the photovoltaic panel and the temperature has an influence on its performances, the *saturation current* can be calculated as

$$I_D = I_{rs} \cdot \left(\frac{T}{T_{ref}} \right)^3 \cdot exp\left[\frac{Ego}{n \cdot V_T} \cdot \left(1 - \frac{T}{T_{ref}} \right) \right] \quad (2.5)$$

Where
$I_{rs} = Reverse\ Saturation\ Current$
$Ego = Band\ gap\ energy\ for\ seminconductor$
$n = Ideal\ factor\ of\ the\ diode$
$V_T = Thermal\ Voltage$

The *Reverse Saturation Current* represents the *Saturation Current* at the temperature reference. The *Reverse Saturation Current* is obtained when the circuit is opened between the diode and the *shunt resistance* and using the equation 2.1:

$$I_{rs} = I_{sc} \frac{1}{exp\left(\frac{V_{OC}}{N_s \cdot n \cdot V_T} \right) - 1} \quad (2.6)$$

Where
$I_{sc} = Short\ Circuit\ Current\ of\ a\ cell$
$V_{OC} = Open\ Circuit\ Voltage\ of\ a\ cell$
$n = Ideal\ factor\ of\ a\ diode$
$V_T = Thermal\ Voltage$

In severel of the above-mentioned equations, we defined the *Thermal Voltage* V_T which represents the links between the flow of electrical current and electrostatic potential across a p-n junction and can be calculated as

$$V_T = \frac{k_B * T}{Q} \tag{2.7}$$

Where
$k_B = Boltzmann\ constant\ 1{,}38 \cdot 10^{-23}\ J/K$
$Q = Charge\ of\ an\ electron\ 1{,}6 \cdot 10^{-19}\ Coulombs$

Now that the equations have been described, it is mandatory to see the functioning curves that practically describes how the different variables interact and impacts the performances of the photovoltaic panels.

2.4 IV and PV Curves

From the previous section, the current can be computed to give a complex relation of the current which depends on many variables:

$$I = \left[I_{sc} + K_i \cdot \left(T - T_{ref}\right)\right] \cdot \frac{I_{rr}}{I_{r0}} - I_D \cdot \left[e^{\frac{\frac{V}{N_s} + I \cdot \frac{R_s}{N_p}}{nV_T}} - 1\right] - \frac{V \cdot \frac{N_p}{N_s} + I \cdot R_s}{R_{sh}} \tag{2.8}$$

On this equation, it can be easily noticed that the current depends on the environmental conditions such as the temperature and the solar irradiance, but also on the solar cell characteristics with I_D, R_{sh}, R_s, K_i and n, and last but not least the phovoltaic panel structure with N_s and N_p.

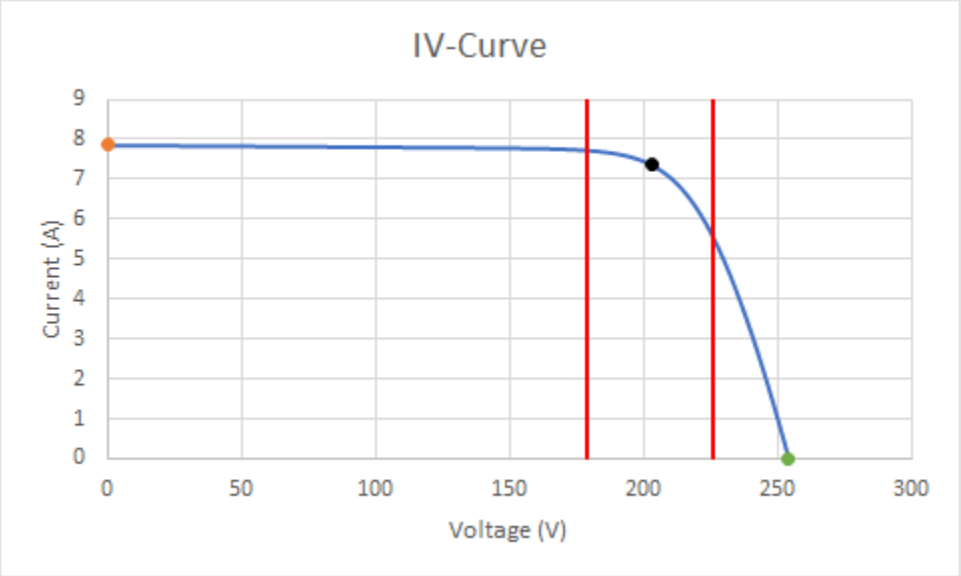

Figure 2.9 IV-Curve T=25°C & Irr=1000W/m²

In Figure 2.9, the plot of the function (2.8) shows that the current is not linear with respect to the voltage. This curve is characterized by three key points.
The first one is the *Short Circuit Current* I_{sc} obtained when the Voltage is null. Secondly, the *Open Circuit Voltage* V_{oc}obtained when the current is null. Lastly, the point that maximizes the power output, the *Maximum Power Point* MPP.
Considering the key point above described, the plot can be divided in three sections: the MPP region, the region on its left side and the region on its right side.
The left-side and the right-side can be approximated as the linear function.

Knowing the current and voltage, we ca obtain the power characteristics through the following formula and the curve is shown in Figure 2.10:

$$P = I * V \tag{2.9}$$

Figure 2.10 shows the Power-Voltage curve and we can see that the key point described in the Current-Voltage curve described earlier have a specific influence on the power curve. The diagram clearly shows that both in conditions of short circuit and open circuit, having respectively the voltage and the current equals to zero, also the power generated in these conditions is null. On the other hand, the MPP as per its name, is the point with the highest power output.

As in the Current-Voltage diagram, three regions can be identified with the same conclusion: 2 linear function approximation for left-side and right-side and the MPP region.

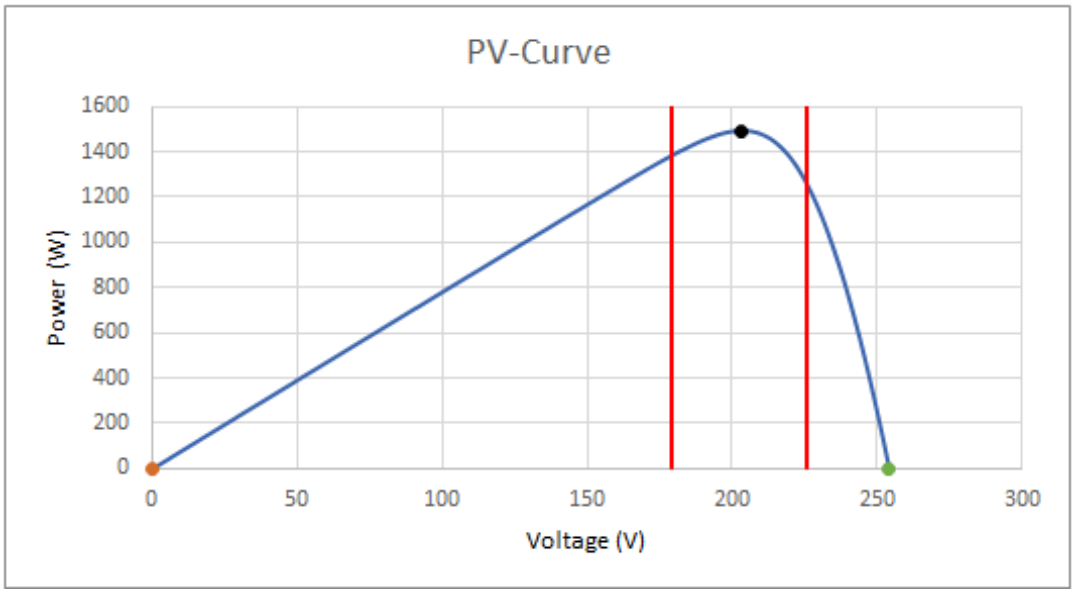

Figure 2.10 PV-Curve T=25°C & Irr=1000W/m²

Figure 2.11 shows the IV-Curve with constant power curves. It shows that only one power curve is tangent to the IV-Curve which is the Maximum Power Point. The others Power curves intersect the IV-Curve in two point, one on the right-side of the MPP region and one on the left-side of the MPP region. It is interesting to notice that the intersect points on the left side are more distance from each other with respect to the ones intersected on the right side. This phenomenon should be remembered for later considerations.

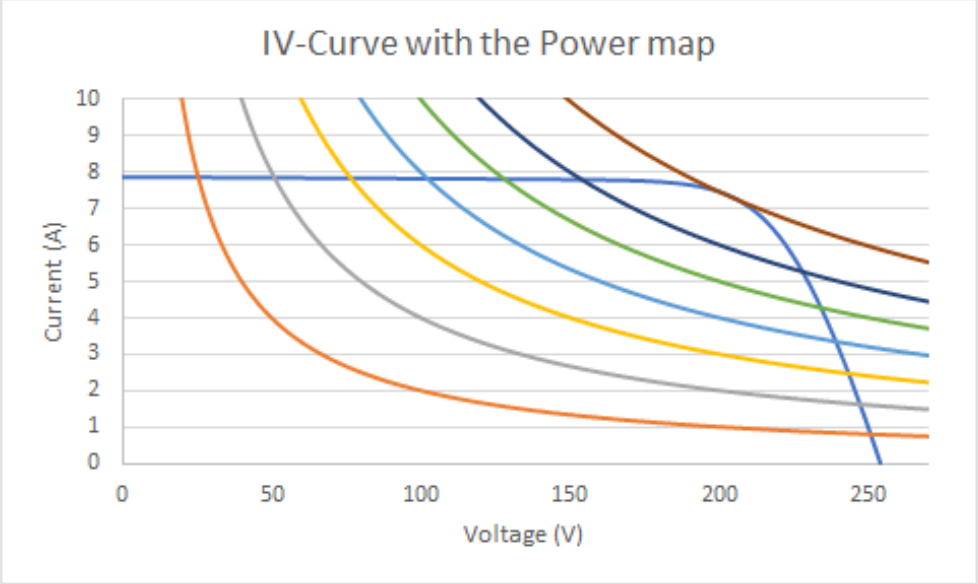

Figure 2.11 IV-Curve with Constant Power Curves

As seen in equation (2.8) and (2.9), the variation of the irradiance and temperature have a considerable impact on the current produced and thus on the power output. This impact can

be seen in Figure 2.12 and Figure 2.13. For the irradiance variation, the I_{SC} is significantly changing, while the V_{OC} is confined in a very close region. There are many factors for this variation such as the hour during a day, seasons and shading. The MPP voltage stays inside a voltage range and some algorithms take this characteristic to improve the tracking [12].

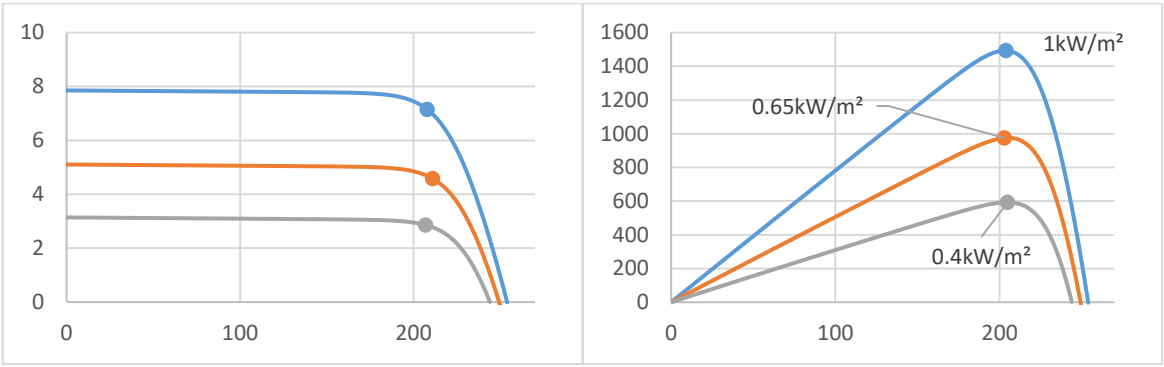

Figure 2.12 IV-Curves and PV-Curves over variation of irradiance

The opposite happens when the Temperature is varying. It happens both when the ambient temperatures change and when the insolation on the cells change. Most of the incident energy is absorbed and converted to heat even if a small amount of the insolation hitting a module is converted to electricity. The I_{SC} is confined in a very close range, whereas the V_{OC} increases when the temperature increases, shifting the MPP to the right, as seen on Figure 2.13. However, the time variation of the temperature is much longer than the time variation of the solar irradiance, and thus for our interest the temperature will have a slow impact in tracking the maximum power point.

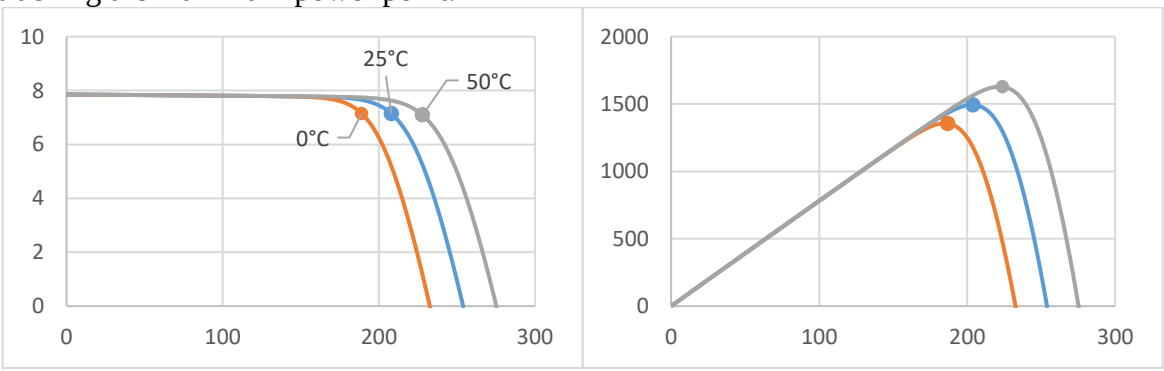

Figure 2.13 IV-Curve and PV-Curve over variation of temperature

To conclude, we have seen how the current can be seen as a function of the voltage and how the two are strictly related when determining the power output and how temperature and irradiance are key variables when determining the variations of the performance curves.
As a consequence, we can also say that the power itself is a function of the voltage meaning that modifying the latter, we can, to a certain extent, control the power output.
The *MPP* research strategies are commonly called *Maximum Power Point Tracking* and can be done through a series of algorithms that are going to be described hereafter.

2.5 MPPT Algorithms

The Maximum Power Point Tracking Algorithms are calculation iterations that are used to find at each instant the voltage and/or current conditions that maximize the power output. These algorithms are divided into categories according to the strategy they use.
Hereafter a scheme of the four main categories of algorithms that used and that we are going to briefly describe in this chapter

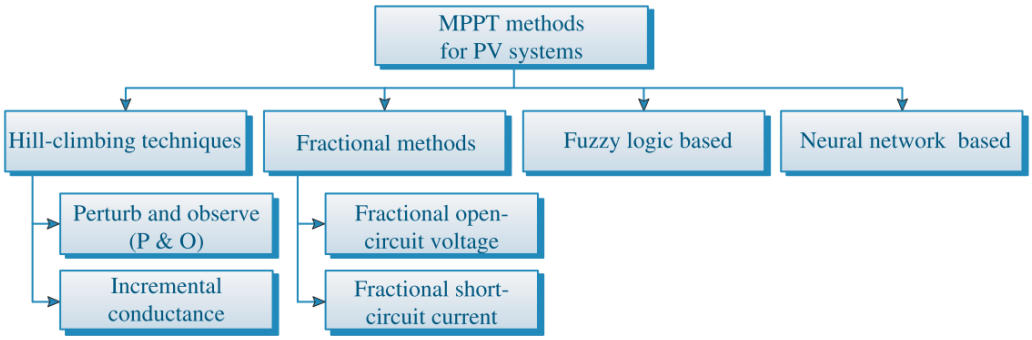

Figure 2.14 MPPT Algorithms Classification [6]

Hill Climbing Techniques:
This category of algorithms is based on the principle of voltage perturbation. At each instant t a perturbation of the voltage is introduce and according to the result obtained and according to the result obtained at the previous instant $t-1$, the algorithm decides if we should perturb the voltage towards the left side or the right side, according to the division of the IV curve seen in the previous chaper. This way, through voltage perturbations, it is possible to stay instant by instant as close as possible to the Maximum Power Point.
Perturb and Observe and Incremental Conductance are the most famous algorithms. Their principles are described on the Figure 2.17 and Figure 2.18. Due to their popularity, many researches have proposed to upgrade and reduce the risk of loosing the tracking as in [12]–[14].

Fractional Methods:
In this category of algorithms, the strategy is based upon a characteristic that has been described during the analysis of the current-voltage curves. In the previous section, we noticed that in the right and left zone, the current-voltage function could be described as linear. Taking advantage of this approximation, the *Fractional Methods* assumes that:

$$V_{MPP} = k \cdot V_{OC}$$
$$I_{MPP} = k \cdot I_{SC}$$

This method's greatest limit is the linear approximation itself since, during operative conditions, the presence of peaks of voltage or current inside the panel will decrease the accuracy of the algorithm.

Fuzzy Logic Based:

This method uses heuristic informations that when repeated in consequent cycles, can determine the *Maximum Power Point*. The inputs are the power variation and voltage variation. The output is the reference voltage variation. To converge to the Maximum power point, different rules are established. Depending on the variation of the inputs, the voltage reference will be determined with a variable step. The method calculation is obtained such as: [15]

$$\begin{cases} \Delta P_{PV} = P_{PV}(k) - P_{PV}(k-1) \\ \Delta V_{PV} = V_{PV}(k) - V_{PV}(k-1) \\ V_{PV-ref}(k) = V_{PV}(k) + \Delta V_{PV-ref}(k) \end{cases}$$

The $\Delta V_{PV-ref}(k)$ is the intersection of the ΔP_{PV} and the ΔV_{PV} calculated inside the following table:

ΔP_{pv}							
ΔV_{pv}	BN	MN	SN	Z	SP	MP	BP
BN	BP	BP	MP	Z	MN	BN	BN
MN	BP	MP	SP	Z	SN	MN	BN
SN	MP	SP	SP	Z	SN	SN	MN
Z	BN	MN	SN	Z	SP	MP	BP
SP	MN	SN	SN	Z	SP	SP	MP
MP	BN	MN	SN	Z	SP	MP	BP
BP	BN	BN	MN	Z	MP	BP	BP

Figure 2.15 Fuzzy logic table [9]

This method gives a faster convergence to the Maximum Power Point.

Neural Network Based:

This last category uses machine learning algorithms to train its neural network through a series of inputs and outputs. The trainging is synthetically composed of:

1) Selecting the inputs: using the inputs given in the database we will be able to compare the outputs return by the algorithm with the real outputs conainted in the database in order to correct the algorithm
2) Determine the outputs: the algorithm will determine the preliminary results that will be compared with the real ones
3) Correction

These three phases briefly describe the training of a machine learning algorithm for *Maximum Power Point Tracking*.

The categories described above, have different approaches but differs as well in their computational cost and thus on their applicability for real operation and their actual cost.
Several studies have been carried to report the different algorithms [3], [5]–[11], and tried to identify their cost-efficiency ratio.
In Figure 2.12 we can appreciate the Energy Generated - Cost diagram exposing some of the most used algorithms for *Maximum Power Point Tracking.*

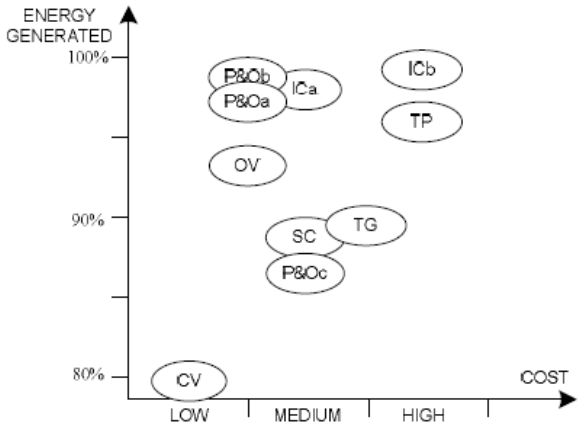

Figure 2.16 Comparison of Cost-Efficiency for different MPPT techniques[16]

Naturally, the most used algorithms will be the ones that maximize the energy generated while having the minimum cost. For this reason, the Incremental Conductance (Inc Cond) and Perturb and Observe (P&O) algorithms are among the most popular ones given their very high efficiency and high performances.

For P&O and IncCond, two measures are needed: voltage and current of the PV panel. Then different combinations are used and compared to the previous value stored in the system to give a direction of the vector. They are based on the fact that, at the MPP, the derivate of the MPP is null. For the first one, the power is computed and compared to the previous value. Then the voltage is compared and depending on the result, the voltage reference will increase or decrease a predefined step value. For the second one, no power computation is done. The conductance and the incremental conductance of the PV panel are calculated, and the result will give the new voltage reference. Both of those algorithms need a fixed voltage step. The problem with this is, at the equilibrium, oscillation will occur and lots of energy will be lost. Reducing the fixed voltage step will reduce the oscillation but will give a higher risk of losing the tracking of the MPP. Increasing the fixed voltage step will reduce the time of convergence but will increase the oscillations. A trade-off can be made to modify these algorithms to be able to adapt to the fixed voltage step, depending on the convergence or the equilibrium phase.

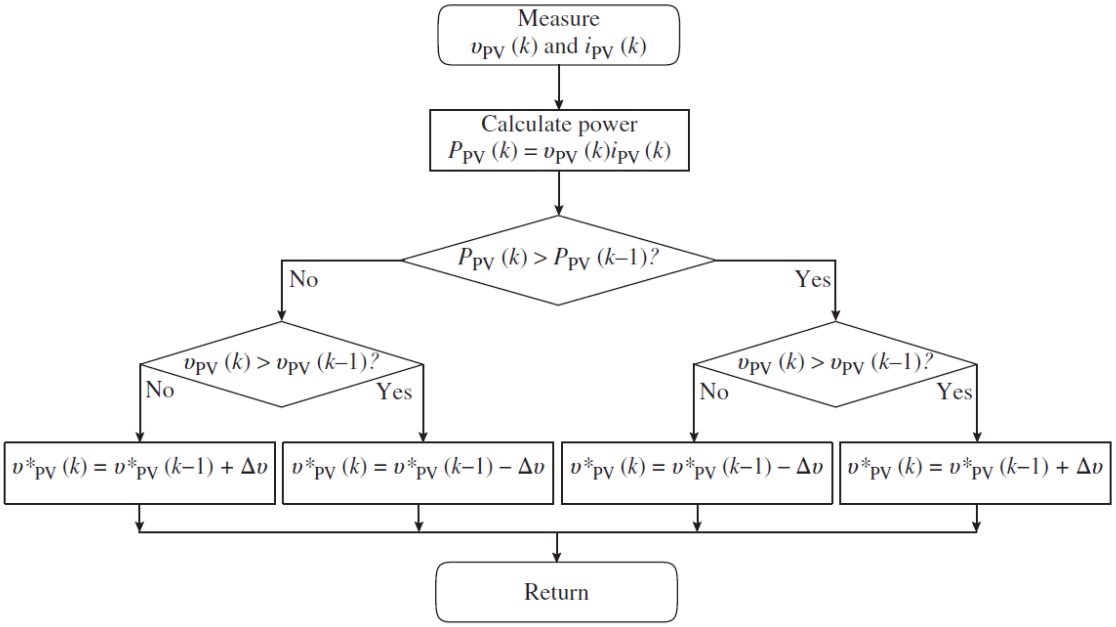

Figure 2.17 P&O Algorithm[6]

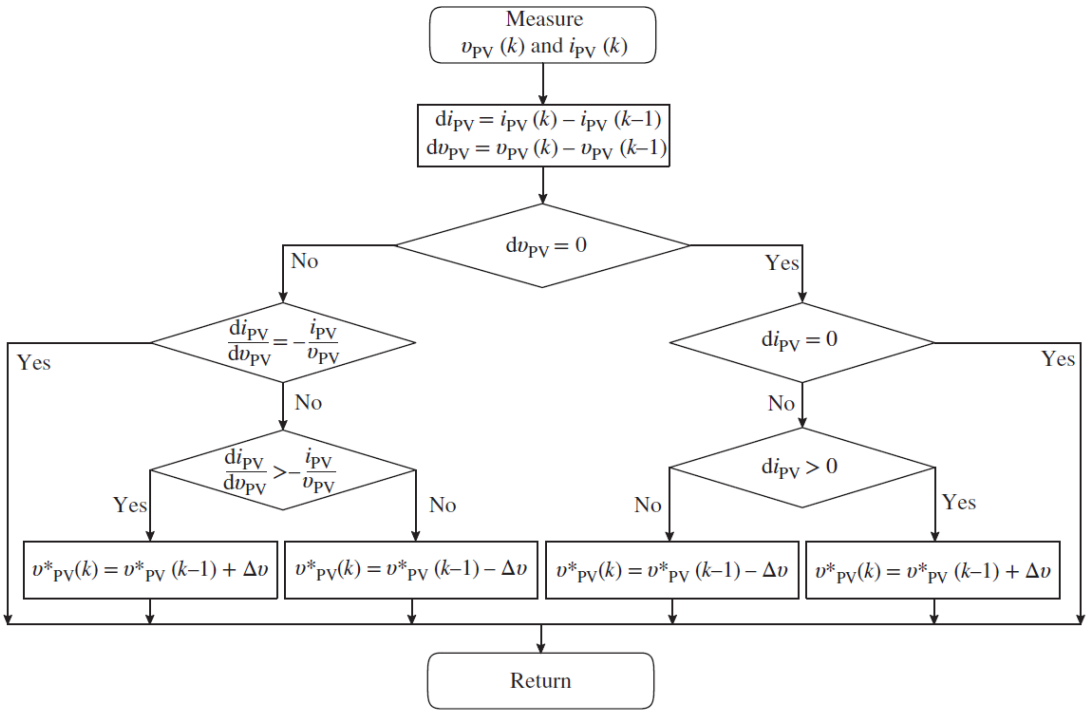

Figure 2.18 IncCond Algorithm [6]

Once the next voltage reference is set, it is introduced as an input for the control system. The output of the system will be the input for a power transfer system, which is in this work a DC/DC converter. Other power transfer systems can be viewed in [9].

2.6 Description of the Control system

Photovoltaic panels are controlled by a power transfer system and a control system. In this section, the boost converter will play the role of the power transfer system because it is the model chosen for this work, but it exists other power transfer system. However they will not be seen here, but they are detailed in [6], [9], [21], [22]. Then the control system used can be defined as an hybrid current mode control, using the sliding mode control in the inner loop.

2.6.3 The boost converter

The Boost Converter is used to control the power of the photovoltaic panel and help to reach the Maximum Power Point thanks to the duty cycle. With a boost converter, the ratio between the input and the output voltages goes from 1 to 0. Thanks to this, it is possible to obtain energy production either when there is low irradiance or when the load power is reduced, which is required for standalone system. The boost converter is directly connected to the PV panel.

The Boost Converter consist of an inductor put in series, then a switcher in parallel, MOSFET, a diode in series, and finally a capacitor *C2* and a resistance *R1* in parallel. The electrical scheme is represented in Figure 2.19. A capacitor *C1* is added between the PV panel and the Boost Converter. This capacitor plays different roles such as to avoid the current pulsed affects the PV panel and to ensure that the current delivered by the PV panel is continuous. *C1* plays a role of filtering and keep safe the PV panel:

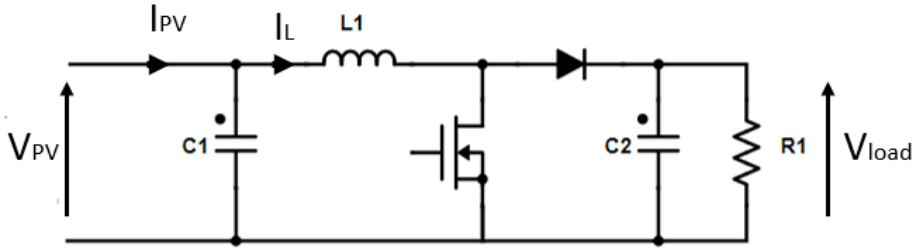

Figure 2.19 PV panel with Boost Converter

2.7 Control system used

Different methods have been developed to control the system and reach the Maximum Power Point. Since the boost converter converts the power, most of the time the duty cycle aims to adjust the output voltage or the input voltage. In the case of searching for the MPP, the duty cycle depends on the ouput voltage and the output current of the PV panel. Even if there are many different strategies [23]–[27], the current mode control appears as the best technology.

2.7.4 Current Mode Control

The Current Control Mode takes two loops. The inner loop stabilizes the current of the inductor while the outer loop consists into giving the inductor current reference. This can be seen on Figure 2.20. Again, the linearization of the Boost Converter is required and has to function around an operating point. The system is thus decomposed into two different transfert functions with the first one using getting the duty cycle due to the inductor current and the second one getting the inductor current reference thanks to the voltage of the PV panel. Then the voltage reference is calculated using the MPPT algorithm and has as input the voltage and the current of the PV panel. Usually the two control systems are proportional integrator controller. Another interesting point is the frequency used for both loops. It is quite obvious that the outer loop needs to give time for the inner loop to converge. But since the voltage reference needs to be calculated to give the best reference point a tradeoff between the frequencies has to be applied so as to not lose the advantages that this solution offers.[23]–[25]

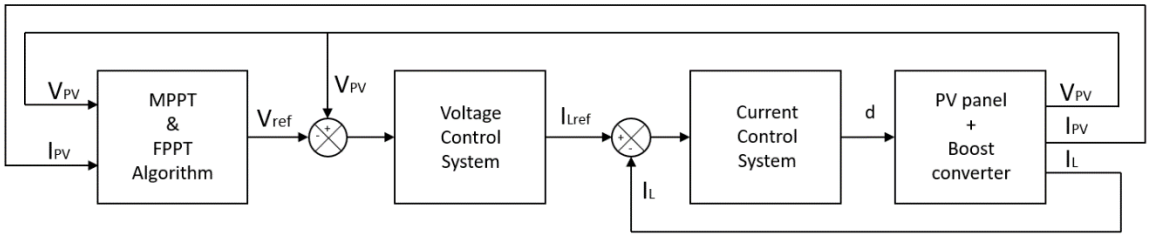

Figure 2.20 Current Control principle

The best solution to control the PV panel and reach the MPP, is to use the sliding mode control in the inner loop and a PI controller in the outer loop. This technique gives a very good result and has no need of linearization. The sliding mode control gives stability, robustness and low error and is quite easy to implement in place. This control principle is therefore essentially based on the use of a discontinuous control intended to maintain the evolution of the system on a switching surface (sliding surface) judiciously chosen. The synthesis must therefore aim to make the sliding surface attractive (condition of attractiveness) from any point in the state space. Once the surface is reached, it is necessary to ensure the sliding along this surface (slip condition) and the stability of the system (stability condition). In other words, it is necessary to find the condition for which the dynamics of the system slides on the surface towards the desired point of equilibrium. On the surface, the dynamics of the system is independent of that of the initial process, which implies that this type of control enters the field of robust controls. These notions of stability are demonstrated by taking into account the principle of stability according to the Lyapunov criterion recalled below [23], [26]-[27]:

$$V: \mathbb{R}^n \to \mathbb{R}^n$$
$$\begin{cases} V(0) = 0 \\ V(x) > 0 \ \forall x \neq 0 \\ \dot{V}(x) \leq 0 \ \forall x \neq 0 \end{cases}$$

The following steps allows to define the equivalent command of the current control.
Choice of surface

$$S = i_L - i_{Lref} \tag{2.10}$$

The lyapunov function

$$V = \frac{1}{2} S^2 \tag{2.11}$$

With function, we obtain the first criteria which is $V(x) > 0 \ \forall x \neq 0$.

And we take the command law as

$$u = \frac{1}{2}[1 - sign(S)] \tag{2.12}$$

Where $sign(S) = 1 \ if \ S < 0$ and $sign(S) = 0 \ if \ S > 0$.

From

$$\dot{V} = \dot{S} \cdot S \tag{2.13}$$

We need to validate the criteria $\dot{V}(x) \leq 0 \ \forall x \neq 0$

From the boost converter circuit, we determine the function $\frac{di_L}{dt}$ as:

$$\frac{di_L}{dt} = \frac{1}{L} \cdot [V_{PV} - V_{load} \cdot (1 - u)] \tag{2.14}$$

After computation, we obtain the following inequation, which fulfilled the criteria:

$$\dot{V} \leq \frac{1}{2} \frac{|S|(\left|V_{load} - 2V_{PV} - 2\dot{i_{Lref}}\right| - V_{load}}{L} \leq 0 \tag{2.15}$$

Then, at the equilibrium, we set $S = 0$, $\dot{S} = 0$ and $u = u_{eq}$. From equation 2.10, and equation 2.14, we compute the equivalent command such as:

$$0 < u_{eq} = \frac{L\dot{i_{Lref}} + V_{load} - V_{PV}}{V_{load}} < 1 \tag{2.16}$$

The equivalent command gives the duty cycle since it is comprised between 0 and 1.

2.8 Objective of this work

Now the different components of the system have been developed, we have a better view of what a photovoltaic system is composed by. It is a very complex system where each part has an impact to the whole system. We have seen that the current technology is made to extract the maximum power of a photovoltaic panel due to the huge losses that occur on the whole system. However to give the opportunity to the photovoltaic system to become half-programmable, we need a variable to control the power produced by the PV panel. Since we have seen that this role is played by the MPPT algorithm, we can modify this algorithm to allow to reduce the power when we need it. The needs come with the load power and thus, it becomes a new input for the MPPT algorithm.

As seen along this chapter, there is only one voltage and current who give the maximum power point. When this MPP is not tracking, two points appears: the left-side point and the right-side point. They are respectively defined in the next chapter as point PA and point PB. The purpose of this work will be to validate that that the point PA is better according to the variation of the solar irradiance and the variation of the load power. Since these two variations can happen very fast, they will be modeled as a step response. Different step responses will be made and study in order to see how the photovoltaic system reacts for the left-side and the right-side.

So the theory of the Reduced Power Point will be developed for each side taking into account the variation of the solar irradiance and the load power. Then the model used will be shown and finally the result of the tests will be discussed.

Chapter 3
Reduced Power Point Tracking

Now that the different parts of the system have been described, the theory of the Reduced Power Point Tracking algorithm will be described taking into account the different effects of the variation of the irradiance and the load power on the system. It is not necessary to see the effect of the temperature, as its effects are not relevant enough at the range of time set up for this study.

3.1 The description of the RPPT

The Reduced Power Point Tracking algorithm provides the solar PV system the flexibility of seperating production from the load. With this algorithm, the solar panels have the possibility to follow the needs and acquire the rank of programmable system. Even though PV power production is strongly dependant on the solar irradiation, RPPT algorithm provides the flexibility to not produce energy then it is not necessary.In order to do separate demand power production from load, the RPPT algorithm must have the capability to reach the MPP if needed but also the capability to converge to the desired power point.
In Figure 3.1, the PV-Curve of a solar panel is represented in black and the load power is represented in blue. Three cases show the different situations that a photovoltaic system is working in operating conditions with an RPPT algorithm. Case A shows the load power higher than the Maximum Power Point of the photovoltaic panel. In that case, it is necessary to work at the MPP and thus use the MPPT algorithm. In case B, the load power equals the MPP, which also conducts to use the MPPT algorithm. In case C, the two curves intersect at two points named as point PA and point PB. PA can also be named as left-side and PB right-side. When the RPPT algorithm is activated, one of these two points can be reached. Assuming that the original state of the PV is at the MPP, if a voltage decrease is required (keeping the power constant) then the point PA must be reached otherwise if a voltage increase is required (keeping the power constant) then PB can be reached.

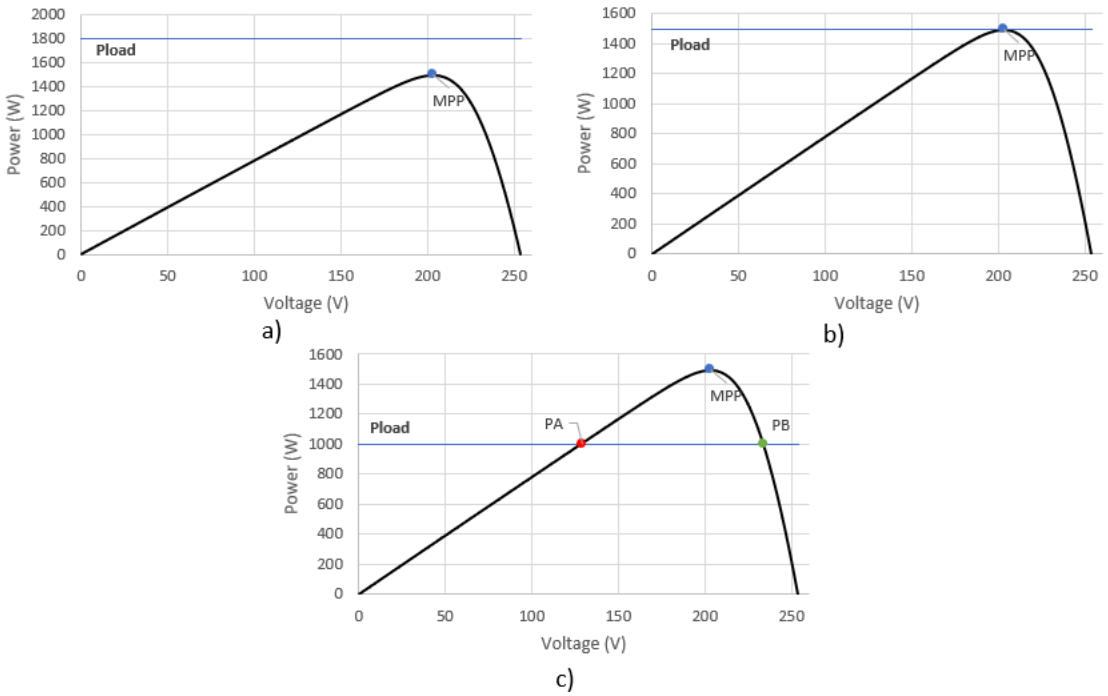

Figure 3.1 PV-Curve with Load Power at different level:
a) $P_{load}>P_{MPP}$, b) $P_{load}=P_{MPP}$, c) $P_{load}<P_{MPP}$

The three cases in Figure 3.1 can happen during the day, which means that the system will have to shift from the Maximum Power Point to the Reduced Power (PA or PB) depending on the variation of the solar irradiance and the load power value. The study of the influence of those variations on the left-side and right-side will show which one of these two points is better according to the precision, stability, robustness and time of response. The next two sections will describe how the RPPT algorithm should react when the solar irradiance varies for the left-side and for the right-side, then when the load power varies.

3.2 Influence of the solar irradiance

As seen in the previous chapter, the solar irradiance varies at each instant and thus changes the PV characteristics shown by the PV-Curve. This variation is very fast and can be modelled as a step response. To be able to discuss on the solar irradiance variation, the load power is kept constant.

3.2.1 Left-side

When the RPPT algorithm is in left-side mode, the voltage will always be comprised between the 0V and V_{MPP}. This sets the power tracking on the long and slow slope of the PV-Curve. It gives the advantage of using a V_{step} like the current MPPT P&O algorithm and helps the system to keep its robustness.

In Figure 3.2 the load power is lower than the Maximum Power Point for this solar irradiance, the system is operating at the point PA using the RPPT algorithm. After a sudden decrease of the solar irradiance, the power is droping fastly, but the voltage is staying the same. Now the load power is higher than the MPP for the new solar irradiance, the RPPT algorithm tries to reach the closest power to the load power. Since it is the MPP, the system will converge to the MPP using the MPPT algorithm. In this case, if the we are in standalone system, the photovoltaic system will have to get a battery to bring the power of the system to the load power.

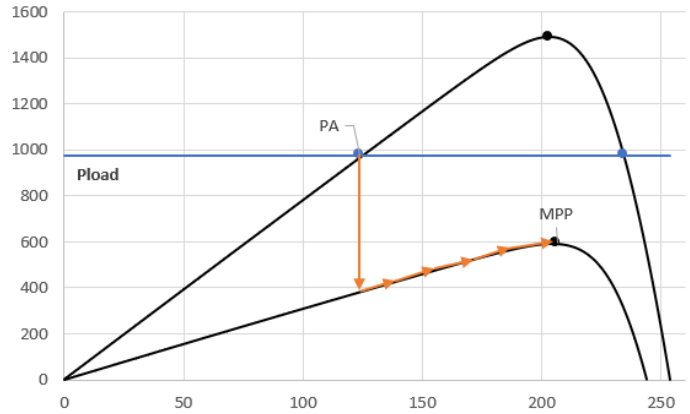

Figure 3.2 Variation of the power from left-side RPP to MPP

In Figure 3.3, the load power is higher than the current solar irradiance. As seen previously, the system is using the MPPT algorithm. After a sudden increase of the solar irradiation, the new power point is moving close to the new MPP. However, this power is higher than the load power. The RPPT algorithm has to converge to the left-side of the MPP, by decreasing the voltage.

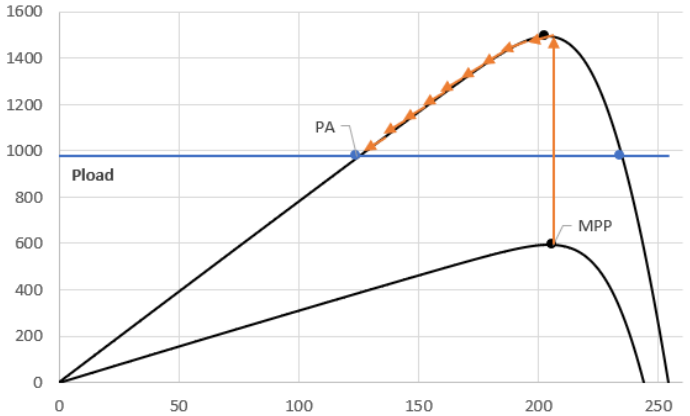

Figure 3.3 Variation of the power from MPP to left-side RPP

In Figure 3.4, the solar irradiance gives an MPP higher than the load power. The system is operating at the point PA_2. After a sudden increase of the solar irradiance, the power of the

system is increasing fastly while the voltage stays the same. Since the new power point is higher than the load power, the RPPT algorithm has to reduce this power by decreasing the voltage and converge to PA_1.

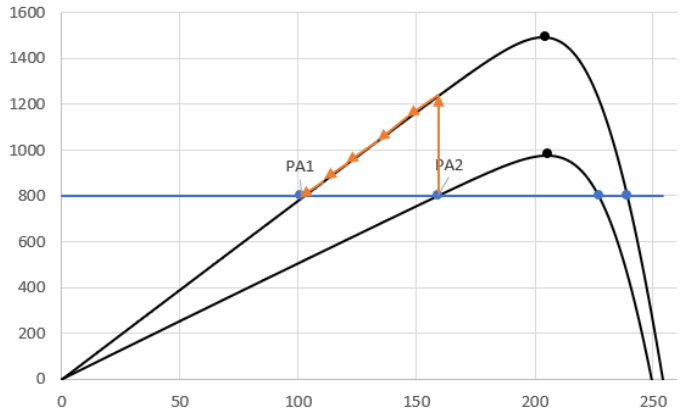

Figure 3.4 Left-side RPPT algorithm after an increase of the irradiance

In Figure 3.5 the solar irradiance gives an MPP lower than the load power. The system is operating at the point PA_1. After a sudden decrease of the solar irradiance, the power of the system has decreased fastly while the voltage stays the same. Since the new power point is lower than the load power, the RPPT algorithm has to increase this power by increasing the voltage and converge to PA_2.

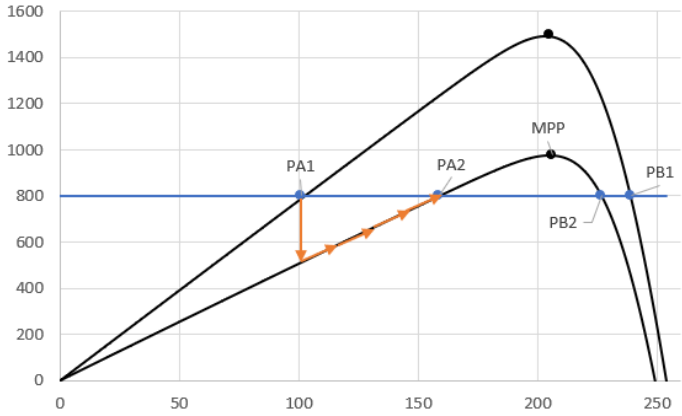

Figure 3.5 Left-side RPPT algorithm after a decrease of the irradiance

It has to be noticed that the different figures show a small variation of the solar irradiance (Figure 3.4 and Figure 3.5) and a large variation of the solar irradiance (Figure 3.2 and Figure 3.3). Also, the difference of the voltage in steady state, before and after the step response, shows a large difference.

3.2.2 Right-side

When the RPPT algorithm is in right-side mode, the voltage will always be comprised between the V_{MPP} and V_{OC}. This sets the power tracking on the short and fast slope of the PV-Curve. The system has an higher risk to lose the tracking and to get a higher variation of the power during the steady state.

In Figure 3.6, the load power is lower than the MPP given at an initial solar irradiance. The system is operating at the point PB using the RPPT algorithm. After a sudden decrease of the solar irradiance, the power is droping fastly, but the voltage stays the same. Now the load power is higher than the MPP for the new solar irradiance, the RPPT algorithm tries to reach the closest power to the load power. Since it is the MPP, the system will converge to the MPP using the MPPT algorithm by reducing the voltage. In this case, if the we are in standalone system, the photovoltaic system will have to get a battery to bring the power of the system to the load power.

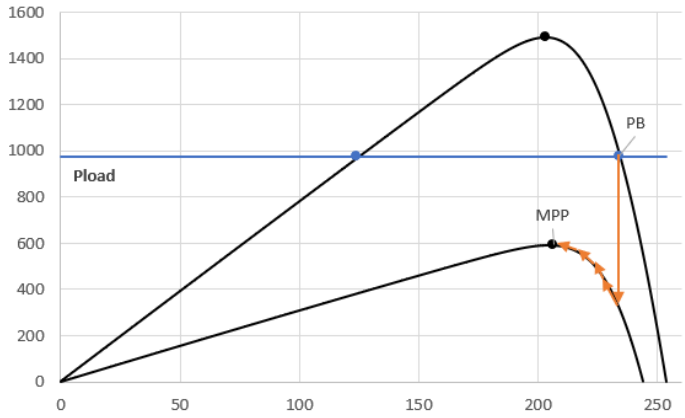

Figure 3.6 Variation of the power from right-side to MPP

In Figure 3.7, the load power is higher than the current solar irradiance. As seen previously, the system is using the MPPT algorithm. After a sudden increase of the solar irradiation, the new power point is moving close to the new MPP. However, this power is higher than the load power. The RPPT algorithm has to converge to the right-side of the MPP, by increasing the voltage.

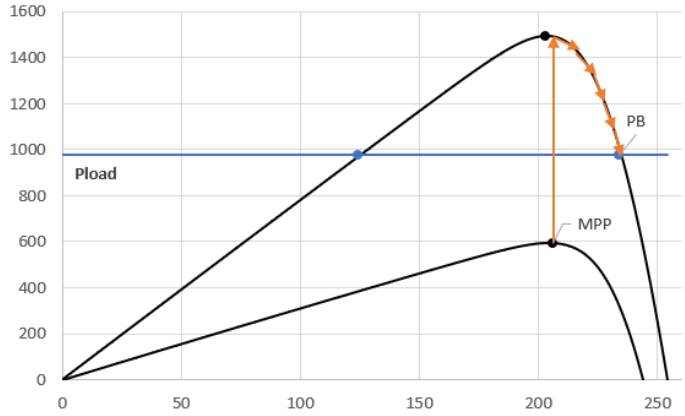

Figure 3.7 Variation of the power from MPP to right-side RPP

In Figure 3.8, the solar irradiance gives an MPP higher than the load power. The system is operating at the point PB_2. After a sudden increase of the solar irradiance, the power of the system is increasing fastly while the voltage stays the same. Since the new power point is higher than the load power, the RPPT algorithm has to reduce this power by decreasing the voltage and converge to PB_1. We can notice that the two steady points before and after the variation are quite close and a peak of power has occurred.

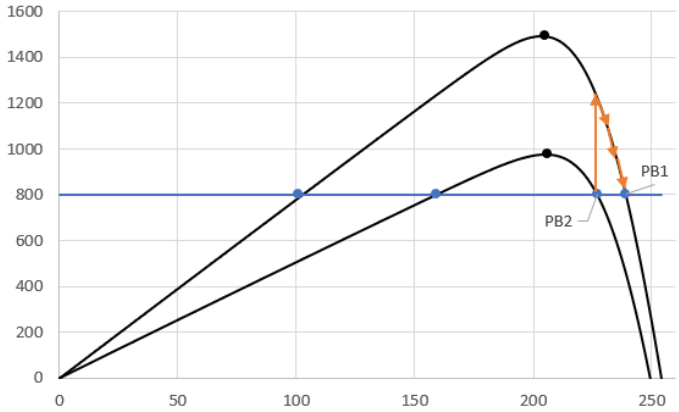

Figure 3.8 Right-side RPPT algorithm after an increase of the irradiance

In Figure 3.9, the solar irradiance gives an MPP lower than the load power. The system is operating at the point PB_1. After a sudden decrease of the solar irradiance, the power of the system has decreased fastly while the voltage stays the same. Since the new power point is lower than the load power, the RPPT algorithm has to increase this power by decreasing the voltage and converge to PB_2.

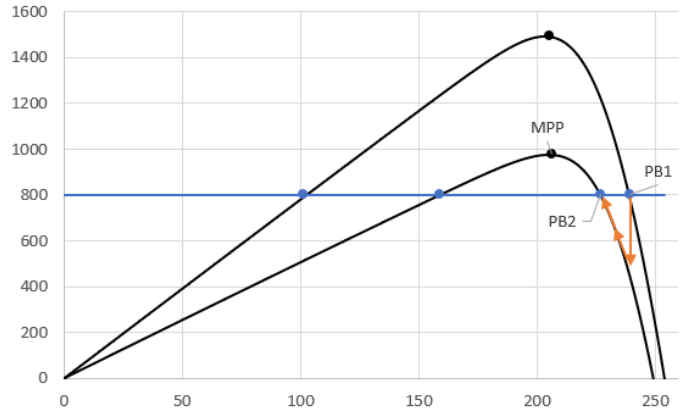

Figure 3.9 Right-side RPPT algorithm after a decrease of the irradiance

Since the voltage operates in a narrow range of voltage, each step has an higher impact on the power. This conducts the system to lose stability and increase the chance to lose the tracking.

3.3 Influence due the required load power

Now the variation of the load power is studied at a constant irradiance. A focus will be made from the MPP to the RPP, describing the different steps that are happening in the IV-Curve and the PV-Curve. Here the V_{step} has been fixed for both cases in order to see the effect on each side.

3.3.3 Left-side

On the left-side, Figure 3.10 shows the PV-Curve and th IV-Curve when the RPPT algorithm moves the system from the MPP to the left-side RPP by reducing the voltage. The first thing that this figure highlights is the number of steps required to converge to the leff-side RPP. It requires 8 steps. Then, looking at the PV-Curve, we see that the system will start to oscillate around this point, but with a small ΔP and a $\Delta V = V_{step}$. If we look at the IV-Curve, we notice that the ΔI is very small which is good due to the control system that we are using. Indeed, the Current control mode is using two loops where the inner one is to control the current and the external loop controls the voltage. It has to be kept in mind that the inner loop runs at a higher frequency than the external loop. So the smaller ΔI is, the faster the control system will converge to the closest value demanded and the chance to lose the track and the stability will be reduced.

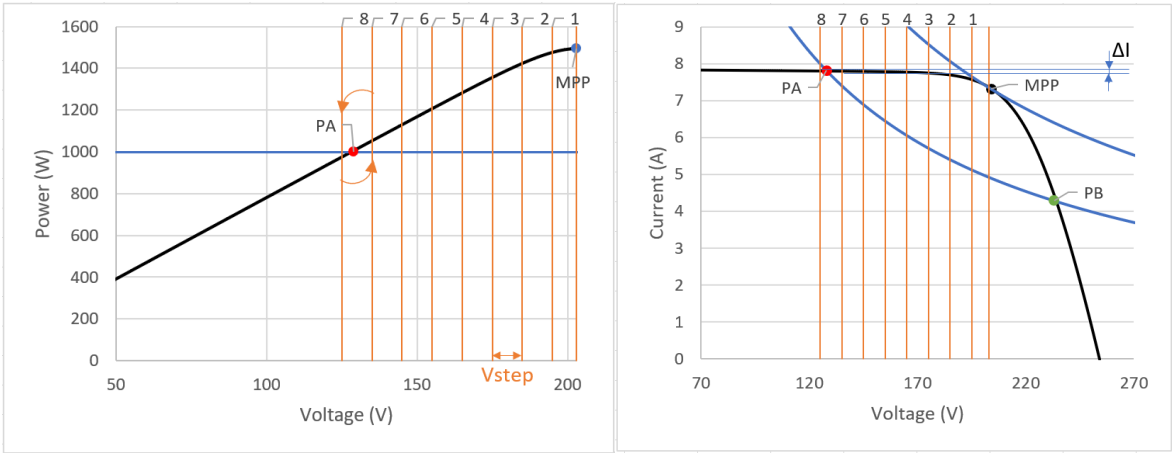

Figure 3.10 PV-Curve and IV-Curve with Convergence to the left-side RPP

3.3.4 Right-side

On the right-side, Figure 3.11 shows the PV-Curve and th IV-Curve when the RPPT algorithm moves the system from the MPP to the right-side RPP by reducing the voltage. The first thing that this figure highlights is the number of steps required to converge to the leff-side RPP. It requires 4 steps, which is twice less than the left-side RPP. Then, looking at the PV-Curve, we see that the system will start to oscillate around this point, but with a large ΔP and a $\Delta V = V_{step}$. If we look at the IV-Curve, we notice that the ΔI is large which is not good due to the control system that we are using. According to what has been seen in the previous section, a larger ΔI will take a longer time for the inner loop to control the current and thus reduce the stability of the system with a higher risk to lose the tracking.

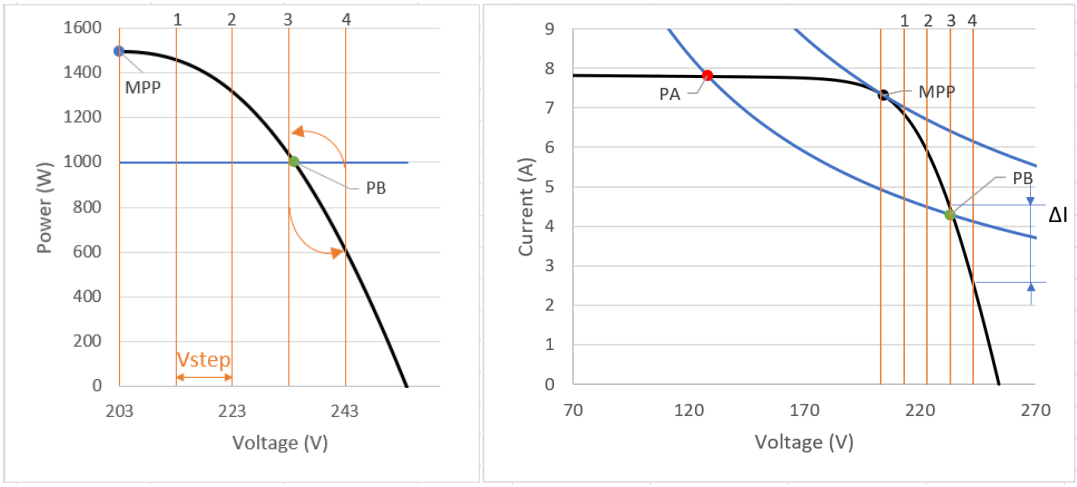

Figure 3.11 PV-Curve and IV-Curve with Convergence to the left-side RPP

3.4 Conclusion

In this chapter, the Reduced Power Point Tracking has been defined. It has highlighted that between the left-side RPP and the right-side RPP, the left-side seems to present a better stability. Even if the time of response is faster on the right-side, it implies to have higher current variation and thus higher power variation inside the photovoltaic system. In order to confirm this, the next chapter will present the model and the different strategies that have been applied during the simulation.

Chapter 4
Simulation Studies

4.1 Base model

The base model is constituted of a PV panel, a Boost Converter and a Control System. In Figure 4.1, the flowsheet of the model has been shown. The PV panel and the Boost converter can be seen as one block developed in Figure 4.2.
In Figure 4.2, the PV panel is connected to a capacitor *C1* added in parallel between the PV panel and the Boost Converter. This capacitor plays different roles such as to avoid the current pulsed affects the PV panel and to ensure that the current delivered by the PV panel is continuous. *C1* plays a role of filtering and keep safe the PV panel. Then the boost converter is modeled with an inductor, a MOSFET, a diode and a capacitor *C2* and a resistance in parallel. For this block, the input variable is the duty cycle δ of the MOSFET. The output values are the voltage of the PV panel, the current of the PV panel and the current of the inductor.
The voltage and the current of the PV panel are the input of the MPPT & RPPT algorithm block plus the load power which is directly defined. The output is the voltage reference V_{ref}. V_{ref} is then compared to the voltage of the PV panel and their difference becomes the input of the voltage control system block. The aim of this block is to transform the voltage reference into the inductor current reference $I_{L\text{-}ref}$ using a proportional integrator.
$I_{L\text{-}ref}$ is compared to the inductor current from the boost converter and their difference becomes the input of the current control system block. The current control system used is the sliding mode control. The output is the duty cycle.

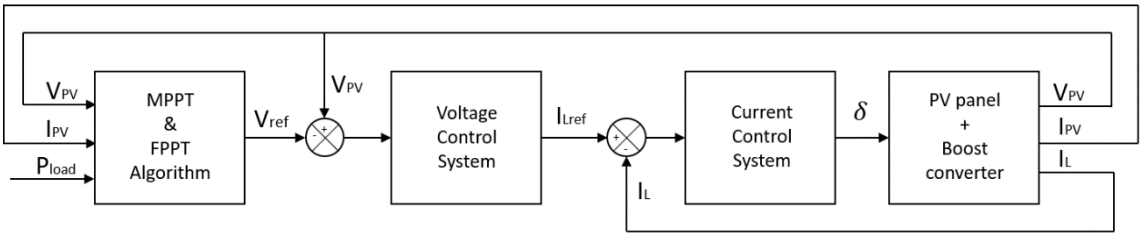

Figure 4.1 Model of the photovoltaic system

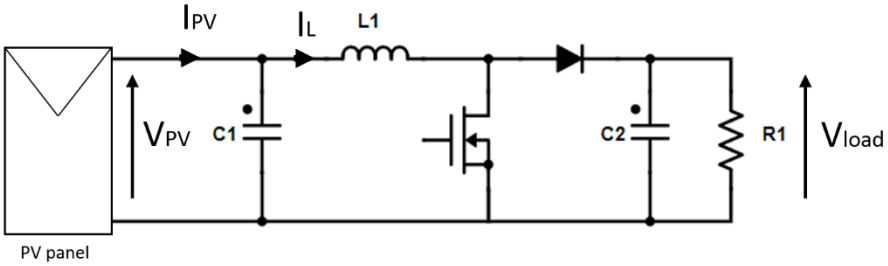

Figure 4.2 Block Scheme of the PV panel + Boost Converter

The Table 4.1 reports the different datas that have been used as the input of the MPPT & RPPT algorithm. It deals with the 3 different situations, which are the maximum power point, the left-side reduced power point and the right-side reduced power point. To run the different simulations, the ΔV is kept the same to evaluate the differences on the result of the simulation.

Table 4.1 Characteristics of the MPPT&RPPT Algorithm

	ΔV (V)	V_{min} (V)	V_{max} (V)	V_{ref} init (V)
MP	0,1	10	300	190
PA	0,1	10	220	130
PB	0,1	150	300	220

The Table 4.2 represents the different frequencies used to simulate the model. The sample frequency f_s defines the sampling frequency of the simulation. Even if it is considered as very high frequency, it represents the number of data calculated during the simulation. Then f_{sc} represents the sampling frequency of the the controlled algorithm. It determines the period to give a new V_{step} to the control system. Finally, the f_{PWM} represents the PWM frequency, which will define the period of time of the MOSFET.

Table 4.2 Frequencies used

Frequencies	f_s (MHz)	f_{sc} (kHz)	f_{PWM} (kHz)
MP, PB, PA	2,5	10	20

Table 4.3 report the two control system characteristics. Whereas the following equations show how the duty cycle is calculated, before it is sent to the boost converter.

Table 4.3 Controller characteristics

Controller	*Gain (V)*	*Ti (s)*
Voltage PI	10	1000
Current	Sliding mode control	

The proportional integrator is defined as

$$i_{L\,ref} = K_p \cdot e + \frac{K_p}{T_i} \cdot \int e\,dt \tag{4.1}$$

Where $e = V_{PV} - V_{ref}$ and represents the voltage error

And the current control system is defined as:

$$0 < \delta = \frac{L \cdot \dot{i_{Lref}} + V_{load} - V_{PV}}{V_{load}} < 1 \tag{4.2}$$

Where δ represents the duty cycle of the boost converter

4.2 Algorithm

The MPPT & RPPT algorithm can be seen in Figure 4.3. It measures the 3 values that are necessary to determine the next V_{ref}, which are V_{PV}, I_{PV} and P_{load}. With the V_{PV} and I_{PV} , the power of the PV panel is determined and then compared to the P_{load}. If $P_{PV} > P_{load}$, the normal conditions are stated and the MPPT algorithm starts. The MPPT algorithm is the P&O MPPT algorithm. Else, it means that the power of the PV panel is higher than the load power and needs to decrease. The RPPT algorithm starts. Before the simulation, the side is selected in order to force the system to shift either to the left-side or the right-side. Depending on this, the new V_{ref} is either increased, if right-side, or decreased, if left-side. Since the ΔV is kept constant, there is no need to update the ΔV.

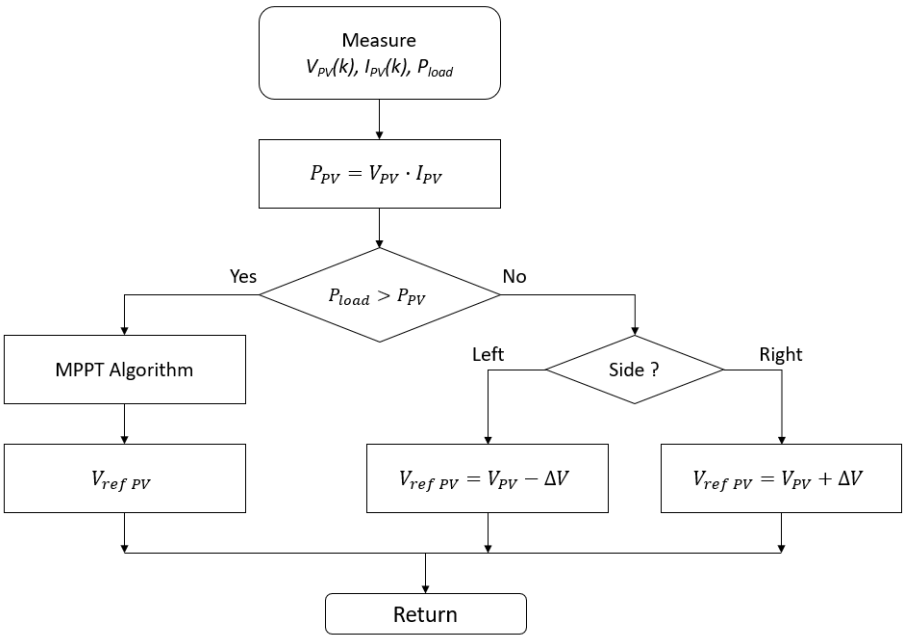

Figure 4.3 MPPT&RPPT Algorithm

4.3 Base case

The first test case studied in this work has no variation for both solar irradiation and power demanded. It is a simulation is used to evaluate the error. It is a test to validate the model and confirm that it gives the results that are expected. Depending on the %error obtained, the other tests can be simulated afterwards. The Table 4.4 gives the input conditions that are used to run the first simulation.

Table 4.4 Initial condition for the 1st simulation

	Irradiation (W/m²)	***Temperature (°C)***	***P_{load} (W)***
Values	1000	25	1000

. The %error at each point and the average % error is found by the formulas given below.

$$\%error_i = \frac{\left|P_{expected} - P_{simu}\right|}{P_{expected}} \tag{4.3}$$

$$\%error_{av} = \frac{\sum \%error_i}{n} * 100 \tag{4.4}$$

In control system, the static error of less than 1% is considered as acceptable.

4.4 Cases with Variation of the solar irradiation

To study the variation with the solar irradiation, first the load power and the temperature are respectively fixed at 1000W and 25°C. Then, 4 cases are considered. They are illustrated in Figure 4.4. The blue curve represents the maximum power available for a solar irradiation variation. The first case is a small step-down response to evaluate how the system reacts when the solar irradiation is reduced slightly, and the system has to converge to a new Reduced Power Point. The second is a small step-up to measure how the system reacts with a slight increase in solar irradiation. The third case is a stronger step-down response, which obliges the system to turn on the Maximum Power Point. It is important to keep in mind that the system needs to keep its ability to run on the previous setup because the RPPT is an evolution of the MPPT and thus, the capacity of the system needs to be able to track the maximum power point when it is needed. So, this case checks the ability for the algorithm to jump from the RPPT to the MPPT without loosing the track. The last case is the opposite of the previous one where strong step up response is introduced in this casesystem moves from search and the track of the Maximum Power Point of MPPT algorithm to the RPPT algorithm. In the similar situation as the third case, this test is important to understand if the new algorithm is able to control and switch between the two algorithms.

This analysis is done because solar irradiation varies continuously at each instant and the step response is the closest simulation to what happens in the reality.

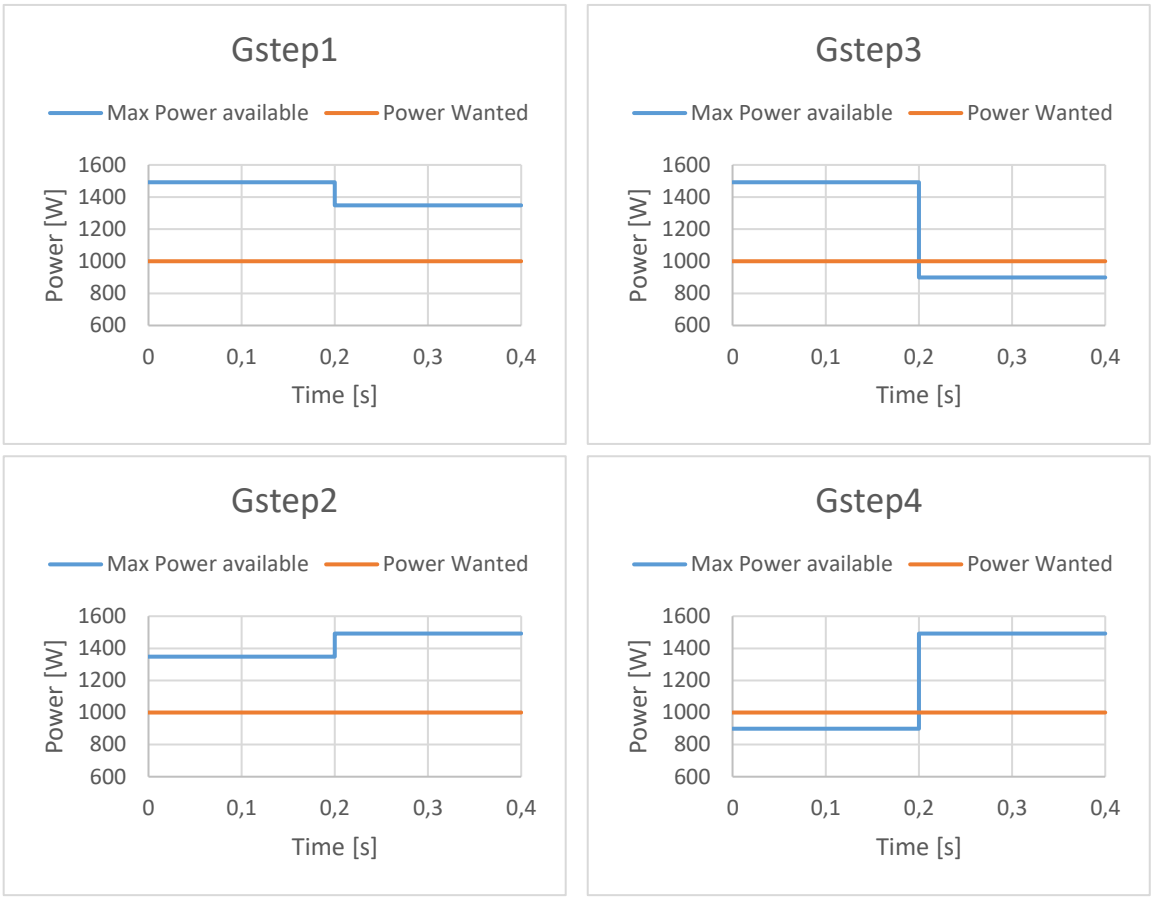

Figure 4.4 Simulation varying the solar irradiance

4.5 Cases with Variation of the required load power

In these cases, the solar irradiation and the temperature are respectively fixed at 1000W/m² and 25°C, which represent a maximum power of about 1493W. The4 cases assumed here are shown in Figure 4.5. The first case is the step-down response, which means that the load power is reduced. Thus, the system is first operating at the maximum power point and then, after the reduction of the load power, it tries to converge to a reduced power point. The second case is a step-up response and helps in analysis how the system reacts whenit jumps from the reduced power point to the maximum power point. These two steps are important as they give an idea about the robustness and the precision of the system. The third case consists of two step-down response to evaluate how low the load power can decrease this helps to check the stability of the algorithm. In this case the system starts from the MPPT algorithm, and then switch on the RPPT algorithm. The last case consists of two step-up response to check the stability of the system. It is important to notice that in island mode, it

does make sense for an installation to require low power during the day, if the installation doesnot need it. Even if it is during a very short time – 0.1ms – it can be important to see if the system is flexible.

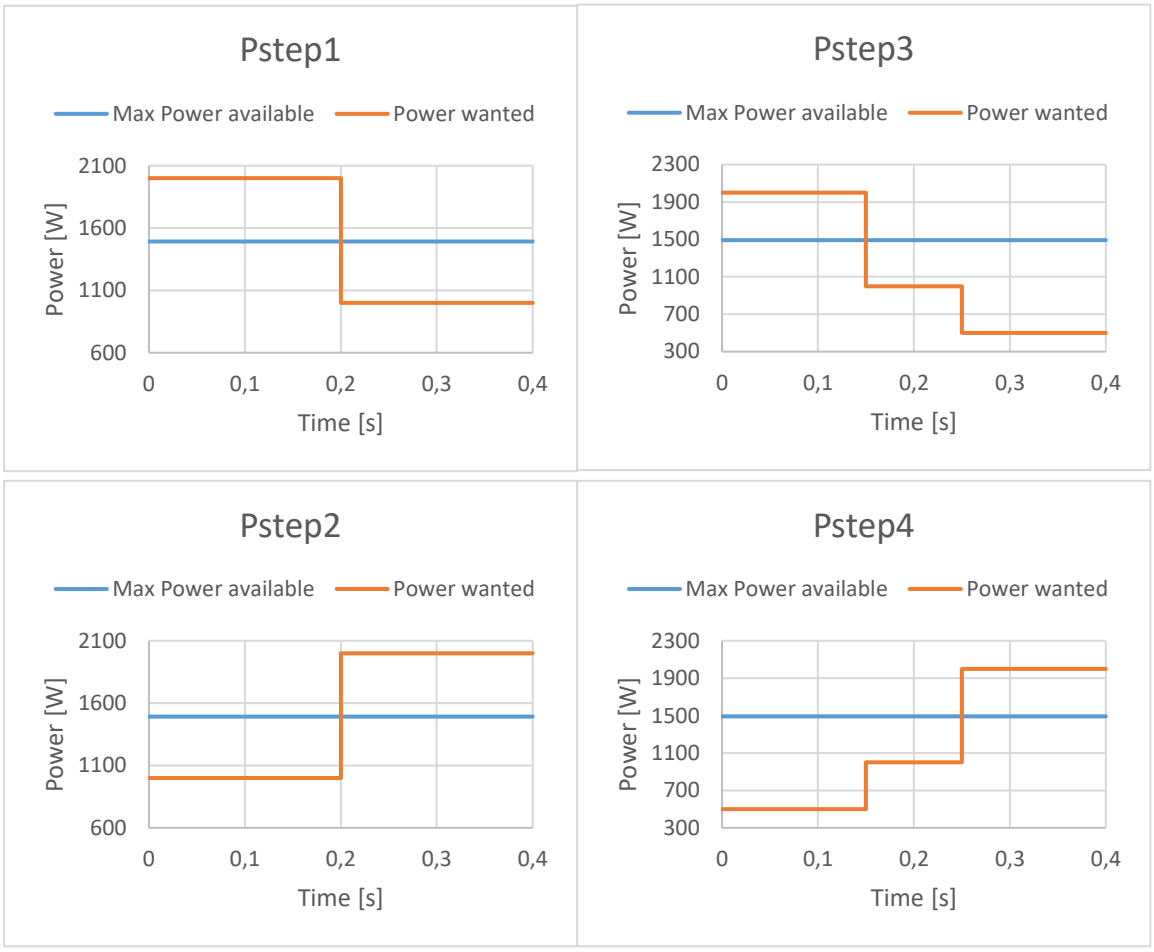

Figure 4.5 Simulation varying the Power of the load

Chapter 5
Results and Discussion

5.1 Simple case

The result of the first simulation can be seen in Figure 5.1. The horizontal axes represents the time in seconds while the vertical axes represents the power in watt. The blue curve represents the left-side RPPT, the red curve represents the right-side RPPT and the dash black curve represents the MPPT. The initial condition had an irradiance of 1000W/m², the temperature at 25°C, which set the MPP around 1493W, and the load power at 1000W. It appears that the response has converged to the expected power. It must be noticed that the first 50ms are not taken into account because they depend on the initial conditions. After zooming to 1000W, the shape of the response shows that the oscillations for the left-side RPP are smaller than the right-side RPP. With the Figure 5.1 and Figure 5.2, it can be seen that the average of the right-side RPP is about 1002W and this average represents the oscillation point.

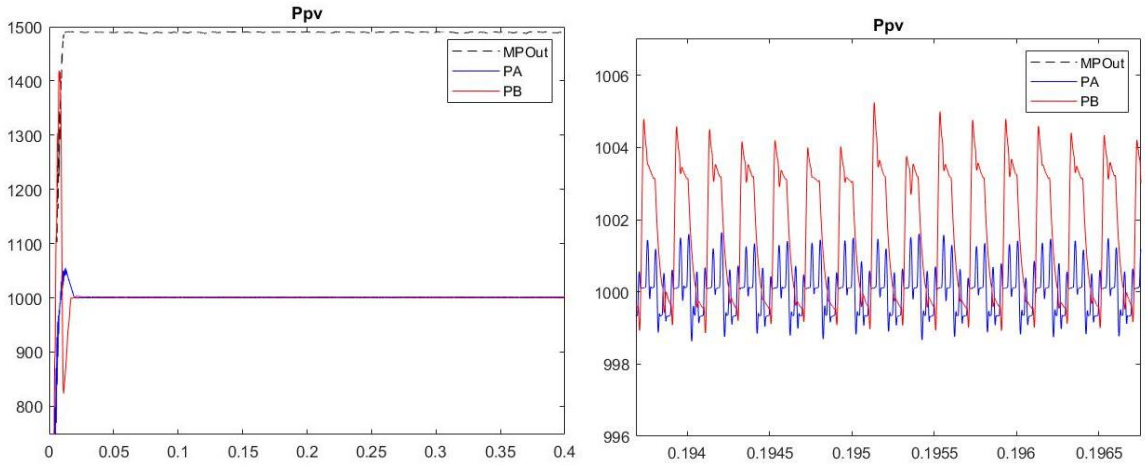

Figure 5.1 Response at constant G=1000W/m² and T = 25°C

In order to get a better value, the $\Delta error$ is represented on Figure 5.2. It is showing that the maximum error is less than 5W and this error is approached when the MPPT algorithm is operating. It does make sense because the maximum power expected was an approximation

from the initial data reported in the characteristics of the PV panel, while the left-side and the right-side have an exact power expected.
Even if on Figure 5.2, the MPP error is higher than the right-side, the expected power is also higher (~+50%). The left-side RPP presents few oscillations and the best convergence. The right-side RPP presents some oscillations, but they are still acceptable. This shows that the MPPT is operating with good accuracy and the RPPT algorithm presents a good precision with a very small static error

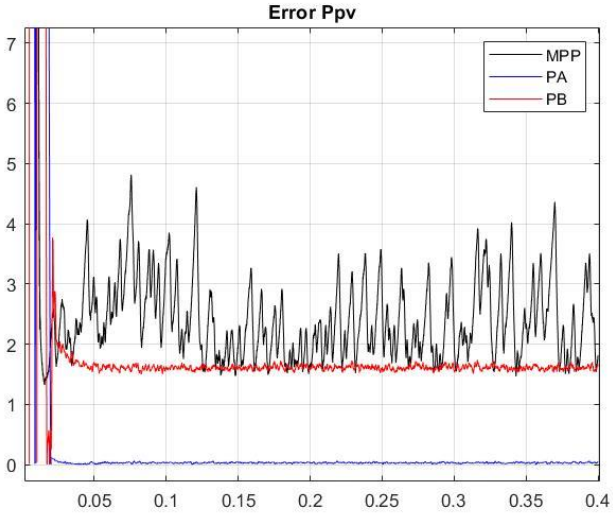

Figure 5.2 Difference between the expected power and the power obtained

Table 5.1 shows the percentage of error:

Table 5.1 Percentage of error

	MPP	***PA***	***PB***
Error %	0,1575%	0,0028%	0,1607%

5.2 Cases with Variation of the solar irradiation

For these tests, the load power and the temperature are kept constant, respectively 1000W and 25°C.

5.2.1 Case 1: Small step-down response

Figure 5.3 shows the small step response. During 0.2s, the irradiance is kept at 1000W/m² and then goes down to 900W/m². This lets the system in the RPPT mode as it can be seen on Figure 5.4.

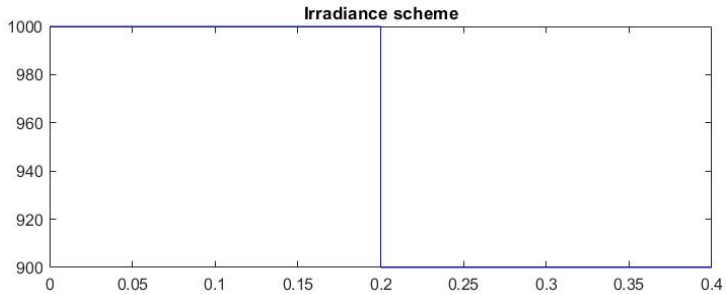

Figure 5.3 Irradiance Case 1: Irradiance scheme

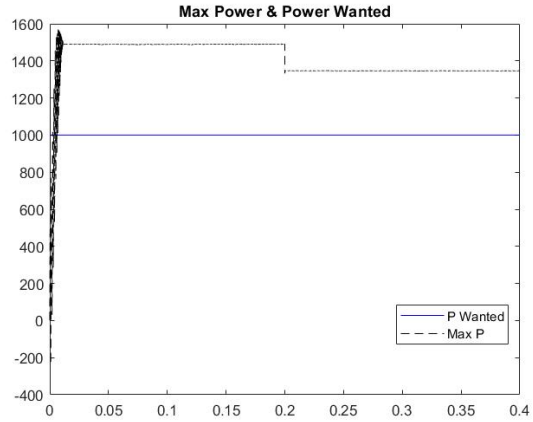

Figure 5.4 Irradiance Case 1: Maximum Power available

Figure 5.5 shows the RPPT response for both left-side and right-side. On the left figure, the response time to reach a stable point is 3ms for right side and for left-side. The right-side has a loss of power during a peak and goes down to 823W but it is able to correct itself very fast, while the left-side goes down to 898W. It must be noted that the oscillation on the right-side are bigger than on the left-side.

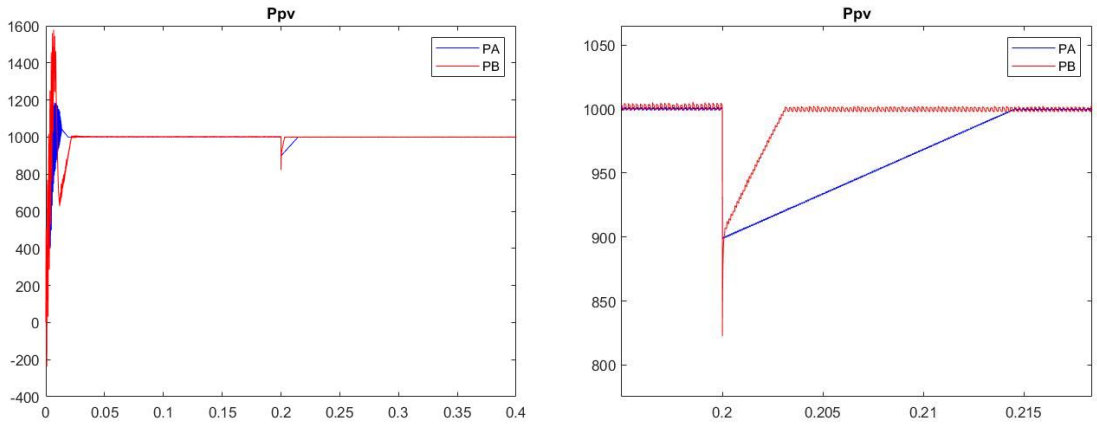

Figure 5.5 Irradiance Case 1: RPPT response

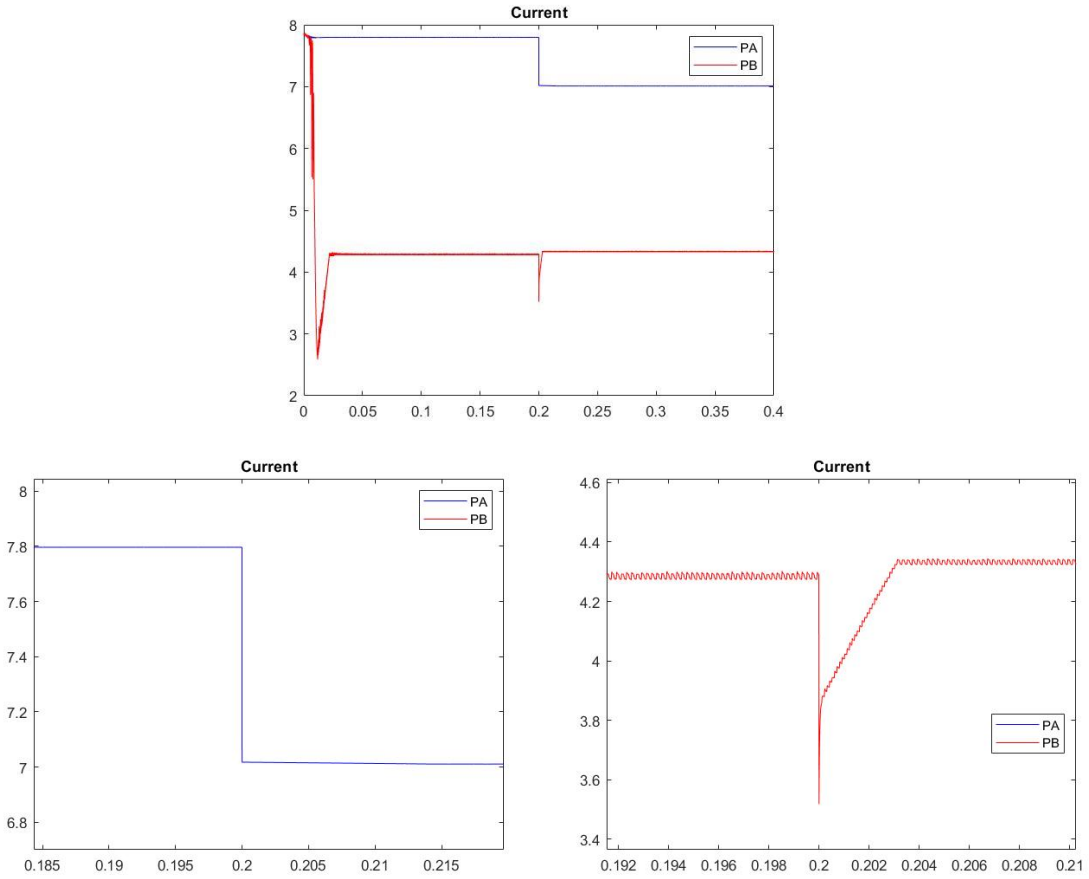

Figure 5.6 Irradiance Case 1: Current

Figure 5.6 shows the current response during the step-down. For the right-side, the current variation is very small from4.28A to 4.33A on average. The peak of power is occurring by the current. Oscillations on the right side are bigger than for the left-side. For the left-side, no oscillation can be seen. The current goes down from 7.8A to 7A.

Figure 5.7 shows the voltage reaction during the simulation. For the left-side, the voltage varies form 128V to 142V. For the right-side, the voltage varies from 233V to 230V on average. No peak can be noticed but still oscillations are present.

Table 5.2 sumarize the main characteristics

Table 5.2 Resume of the Irradiation Case 1

	Left-side	**Right-side**
Peak (W)	898	823
Time (ms)	14	3
ΔI(A)	0.8	0.05
ΔV (V)	14	3

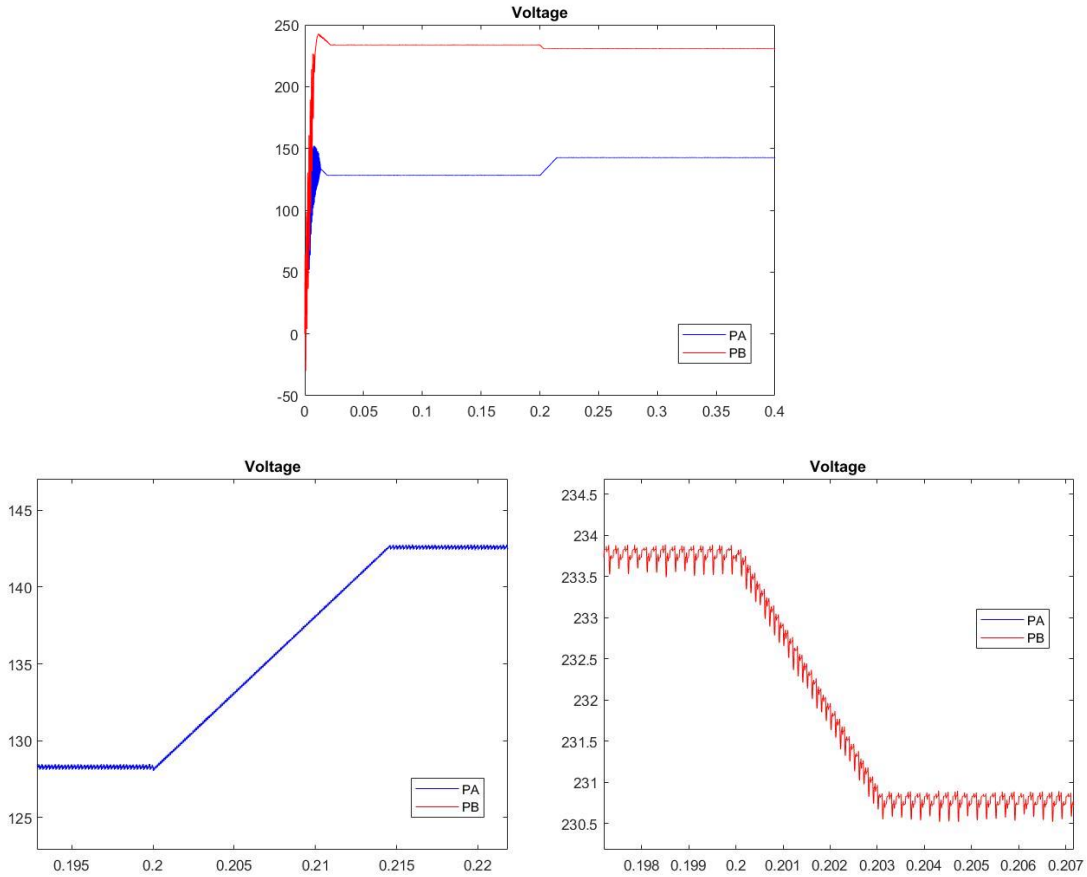

Figure 5.7 Irradiance Case 1: Voltage

5.2.2 Case 2: Small step-up response

Figure 5.8 shows the small step response. During 0.2s, the irradiance is kept at 900W/m² and then goes up to 1000W/m². This lets the system in the RPPT mode as it can be seen on Figure 5.9.

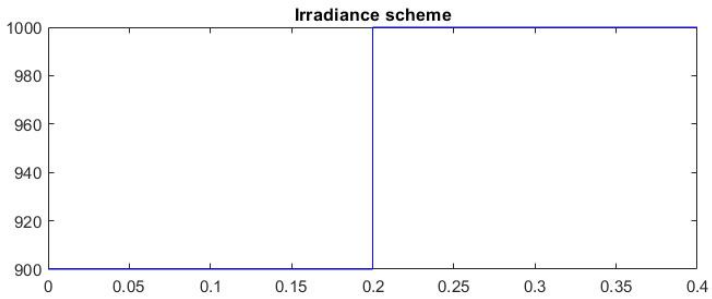

Figure 5.8 Irradiance Case 2: irradiance Scheme

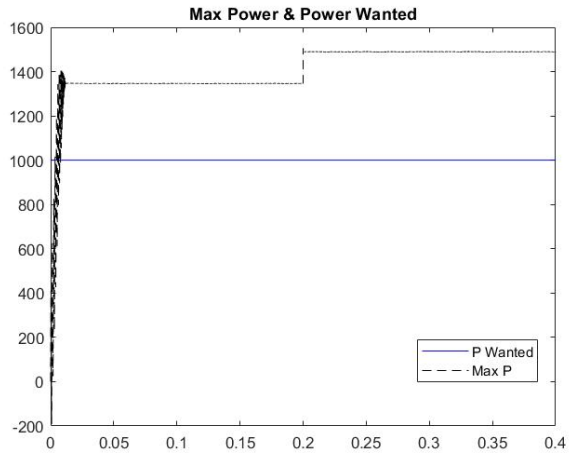

Figure 5.9 Irradiance Case 2: Maximum Power available

Figure 5.10 shows the RPPT response for both left-side and right-side. On the left figure, the time response to stabilize is 3ms and 14ms respectively for right-side and left-side. The right-side has a loss of power during a peak and has a peak to 1179W but it is able to correct very fast, while the left-side goes down to 1114W. It must be noted that the oscillations on the right-side are bigger than on the left-side.

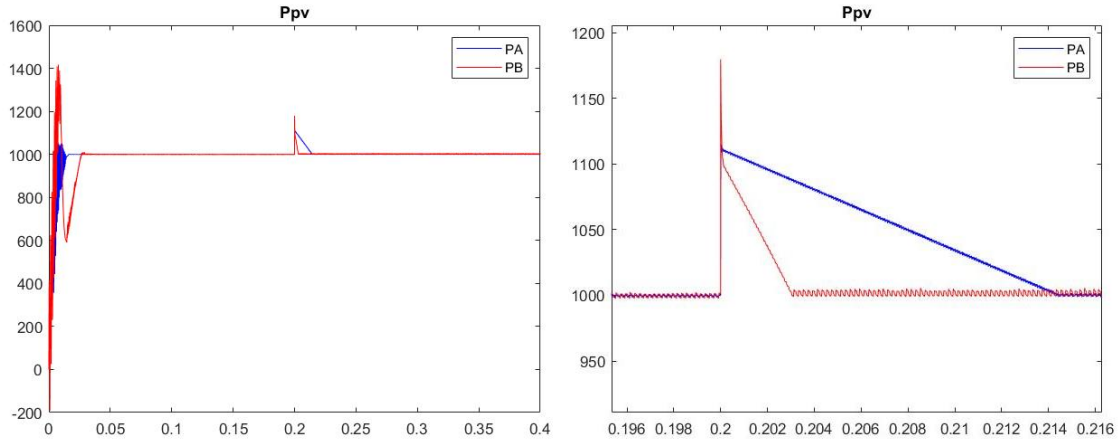

Figure 5.10 Irradiance Case 2: RPPT response

Figure 5.11 shows the current response during the simulation. For the right-side, the current variation is very small from 4.33A to 4.28A on average. The peak of power is occurring by the current. There are osciallations on the right side while for the left-side, no oscillation can be seen. On the left side the current goes down from 7A to 7.8A. This shows that the results make sense because they are the symmetric from the step-down, Case 1.

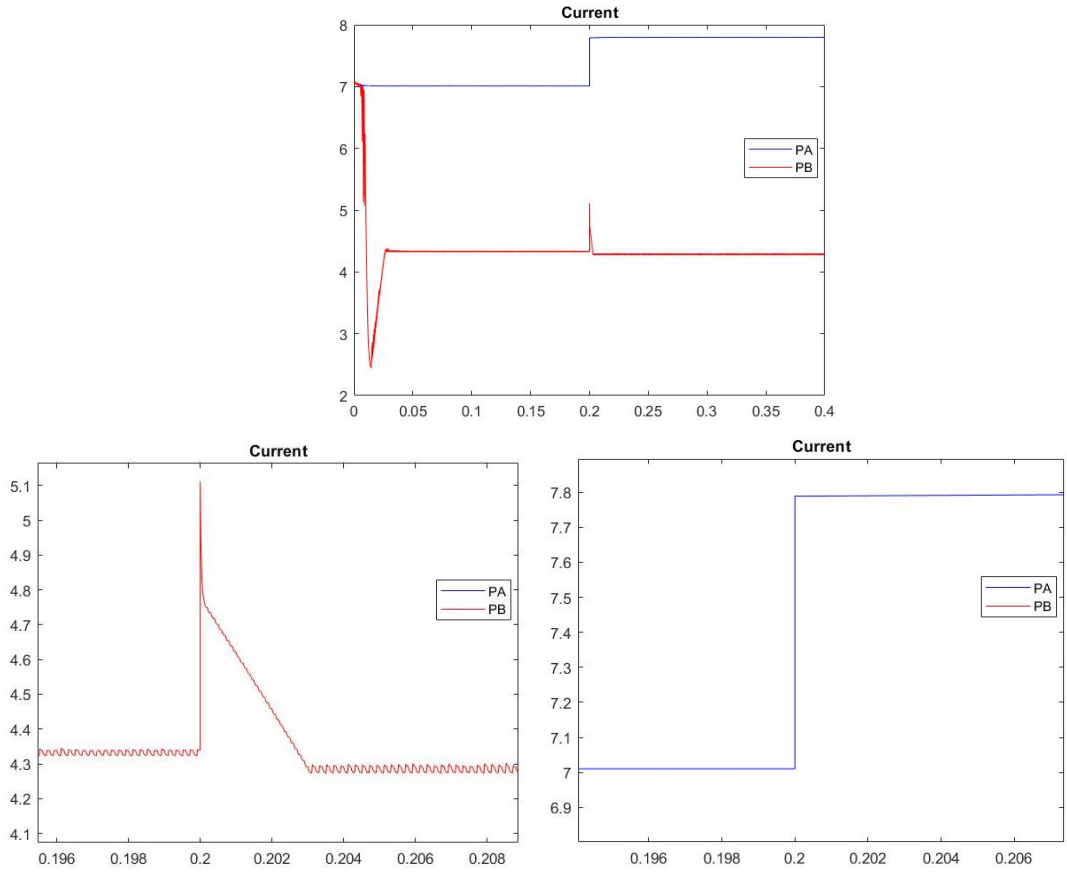

Figure 5.11 Irradiance Case 2: Current

Figure 5.12 shows the voltage reaction during the simulation. For the left-side, the voltage varies form 142V to 128V. For the right-side, the voltage varies from 230V to 233V on average. No peak can be noticed but still oscillations are present. Again, the results make sense because they are the opposite of the previous case.

Table 5.3Table 5.2 sumarizes the main characteristics.

Table 5.3 Resume of the Irradiation Case 2

	Left-side	**Right-side**
Peak (W)	1114	1179
Time (ms)	14	3
ΔI(A)	0.8	0.05
ΔV (V)	14	3

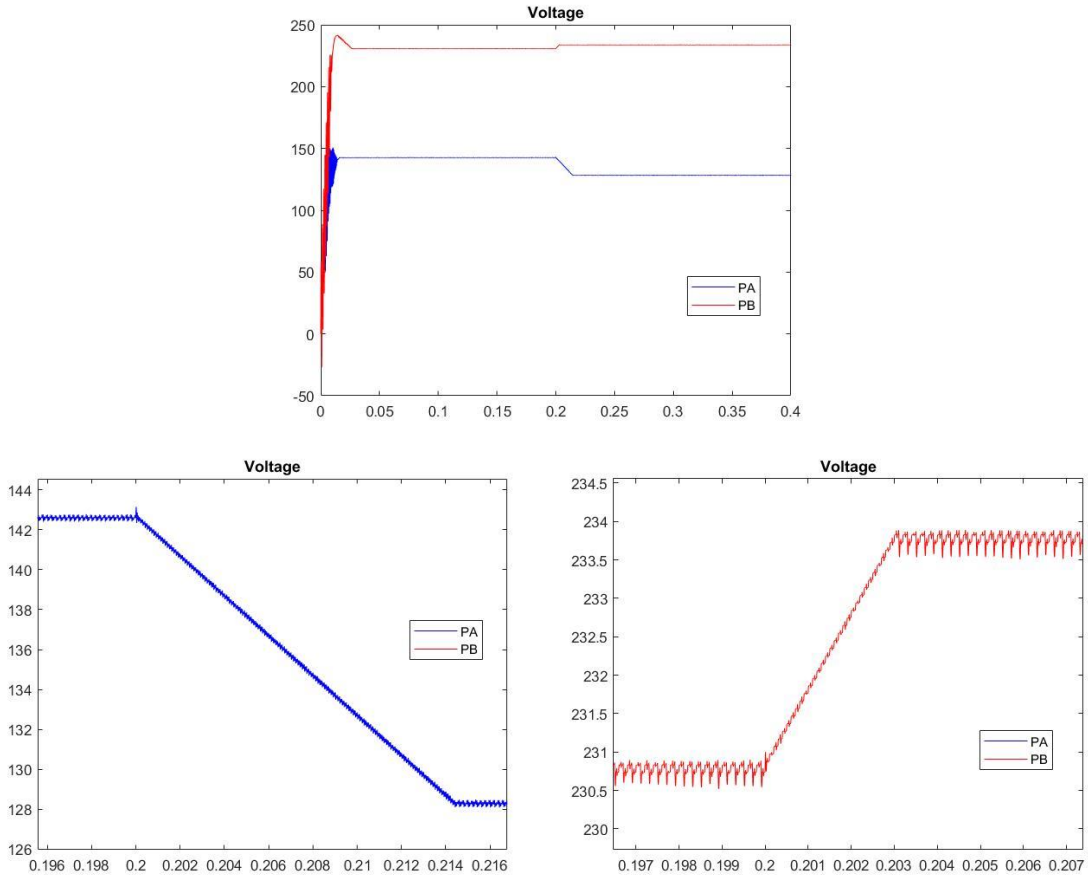

Figure 5.12 Irradiance Case 2: Voltage

5.2.3 Case 3: Big step-down response

Figure 5.13 shows the big step response. During 0.2s, the irradiance is kept at 1000W/m² and then goes down to 600W/m². This drives the system to jump from RPPT mode to the MPPT mode as it can be seen on Figure 5.14.

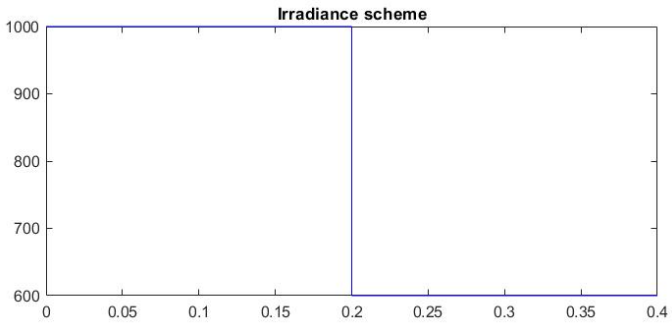

Figure 5.13 Irradiance Case 3: irradiance Scheme

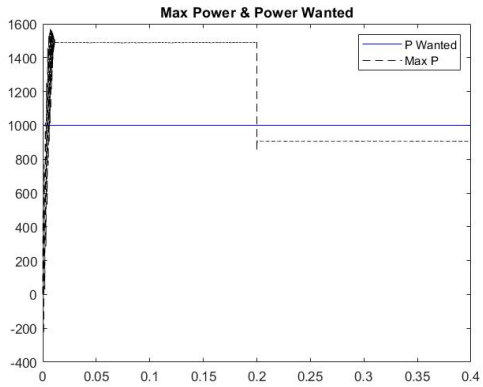

Figure 5.14 Irradiance Case 3: Maximum Power available

Figure 5.15 shows the RPPT response for both left-side and right-side. On the left figure, the time response to stabilize is 28ms and 74ms respectively for right-side and left-side. The right-side has a loss of power during a peak and has a peak to 280W but it is able to correct itself very fast, while the left-side goes down to 600W. It must be noted that the oscillations on the right-side are bigger than the oscillations on the left-side. Some oscillations are occur when the step down is happening, but the tracking is able to correct the trajectory very fast. From both sides, the system can reach the MPP.

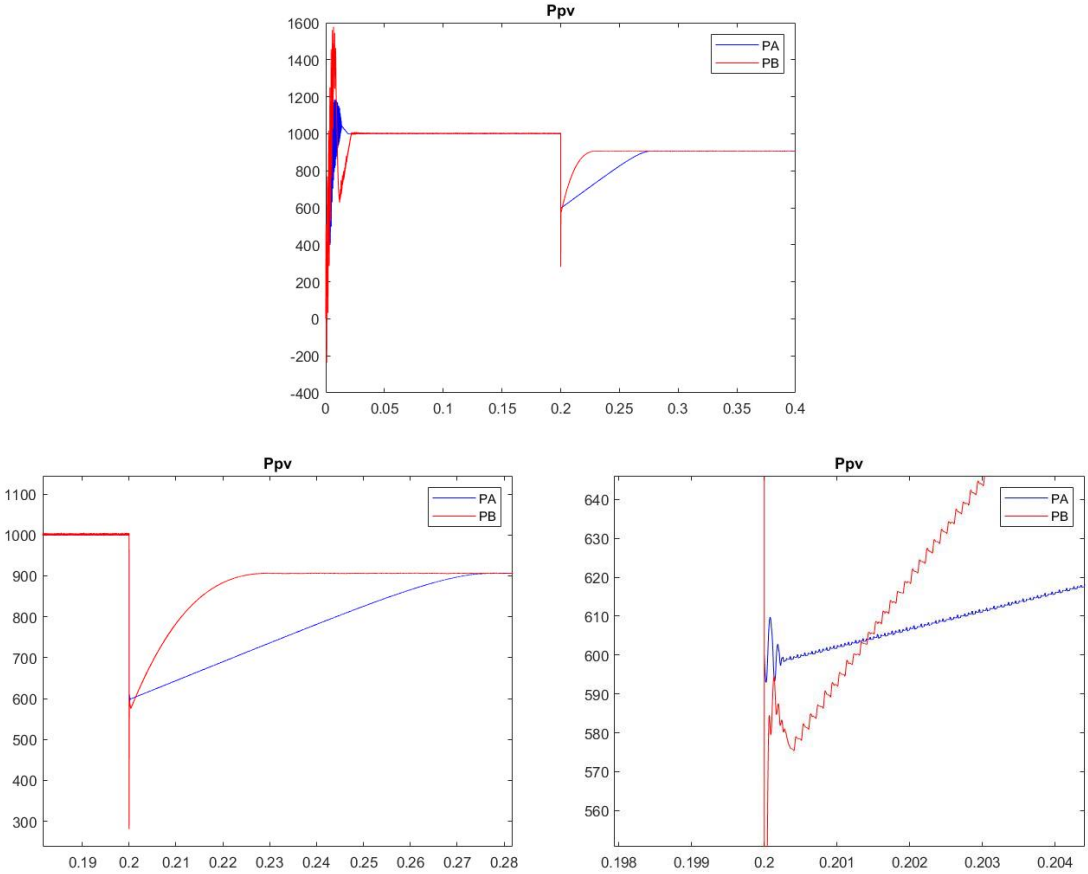

Figure 5.15 Irradiance Case 3: RPPT response

Figure 5.16 shows the current reaction during the simulation. For the right-side, the current variation is very less from 4.29A to 4.4A on average. The peak of power is occurring by the current and is 1.2A. On the right side there are oscillation while for the left-side, no oscillations can be seen but there are 2 phases. In the first phase, the current goes from 7.8A to 4.68A and is effectuated very fast, it is due to the loss of irradiance and the algorithm does not have the time to counter this loss. The second phase converges to 4.4A but starts after 48ms.

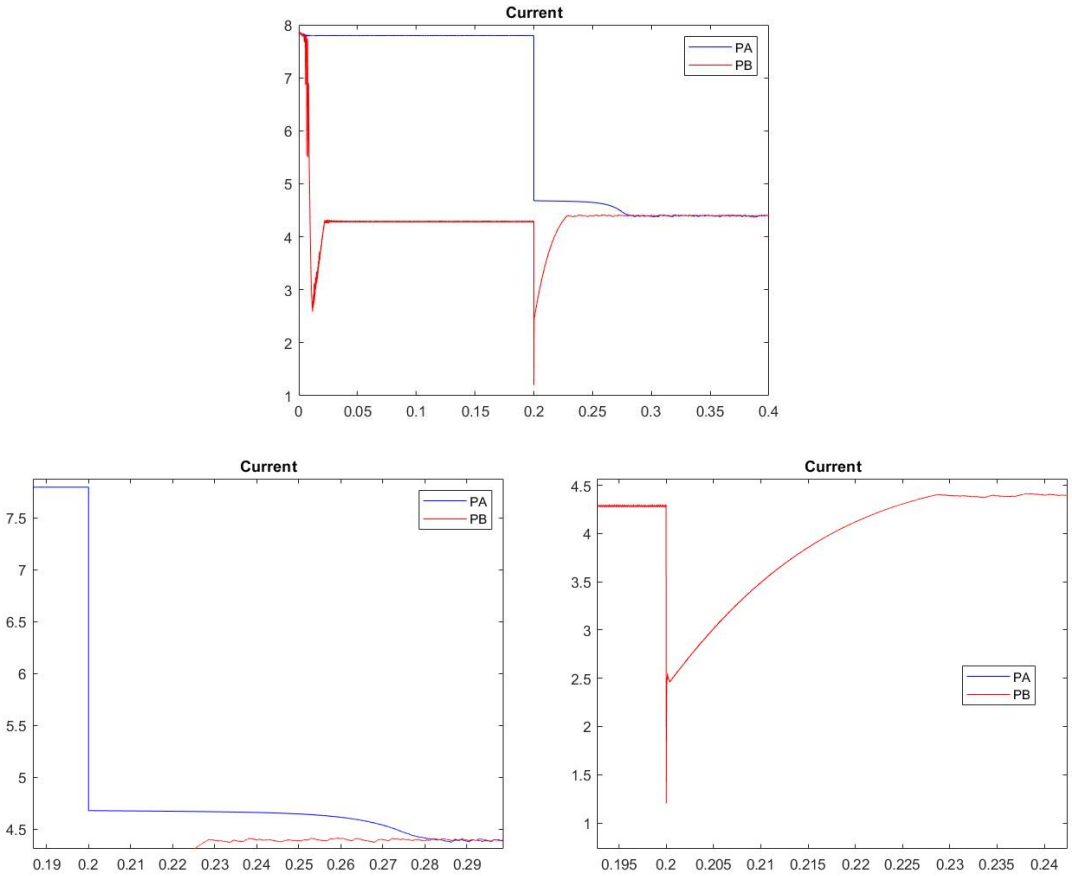

Figure 5.16 Irradiance Case 3: Current

Figure 5.17 shows the voltage reaction during the simulation. For the left-side, the voltage varies form 128V to 206V. For the right-side, the voltage varies from 233V to 206V on average.

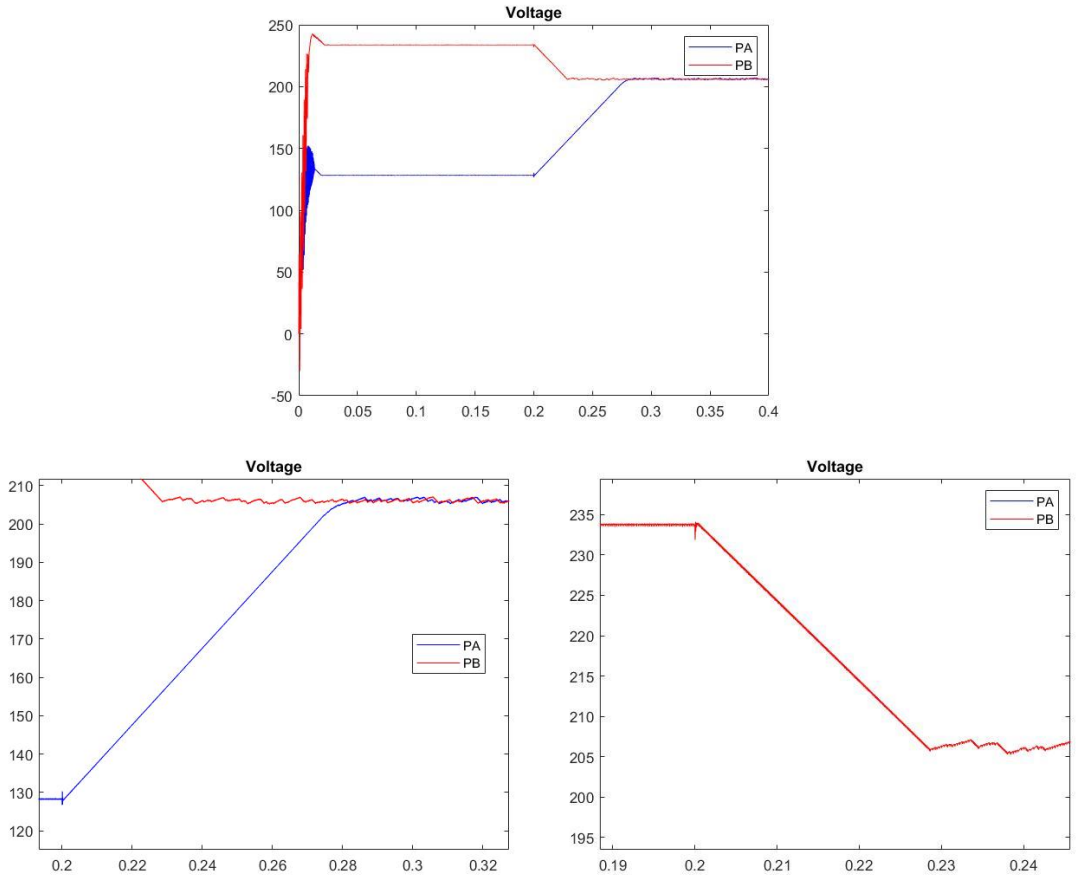

Figure 5.17 Irradiance Case 3: Voltage

Table 5.4 and Table 5.2 sumarizes the main characteristics.

Table 5.4 Resume of the Irradiation Case 3

	Left-side	**Right-side**
Peak (W)	600	280
Time (ms)	74	28
ΔI(A)	3.4	0.11
ΔV (V)	78	27

5.2.4 Case 4: Big step-up response

Figure 5.18 depicts the big step response. During 0.2s, the irradiance is kept at 600W/m² and then goes up to 1000W/m². This drives the system to jump from MPPT mode to the RPPT mode as seen on Figure 5.19.

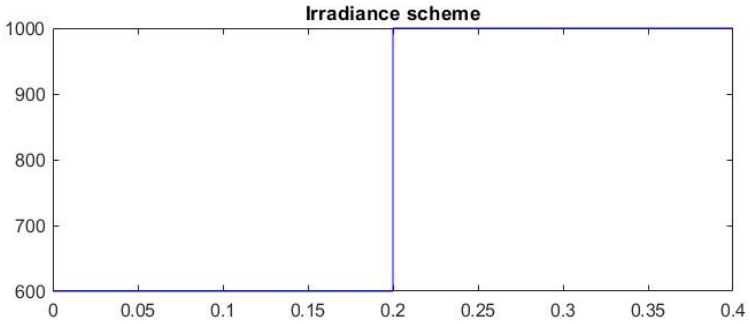

Figure 5.18 Irradiance Case 4: irradiance Scheme

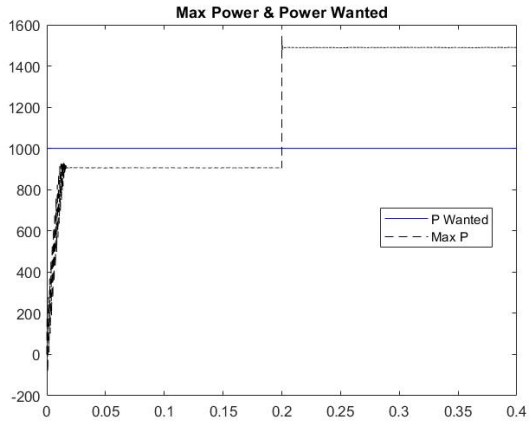

Figure 5.19 Irradiance Case 4: Maximum Power available

Figure 5.20 shows the RPPT response for both left-side and right-side. First the two simulations are on MPPT mode, then the due to the increase of the irradiance a power peak appearsr and the RPPT mode is activated. On the left figure, the time response to stabilize is 28ms and 79ms respectively for right-side and left-side. The right-side has an increase of power during a peak and has a peak of 1547W but it is able to correct itself very fast, while the left-side goes to 1489W. It has to be noticed that the oscillations on the right-side are bigger than on the left-side. Some oscillations are occur when the step down is happening, but the tracking is able to correct the trajectory very fast. From both sides, the system can reach the RPP. The peaks represent the point on the PV-Curve between the two irradiances.

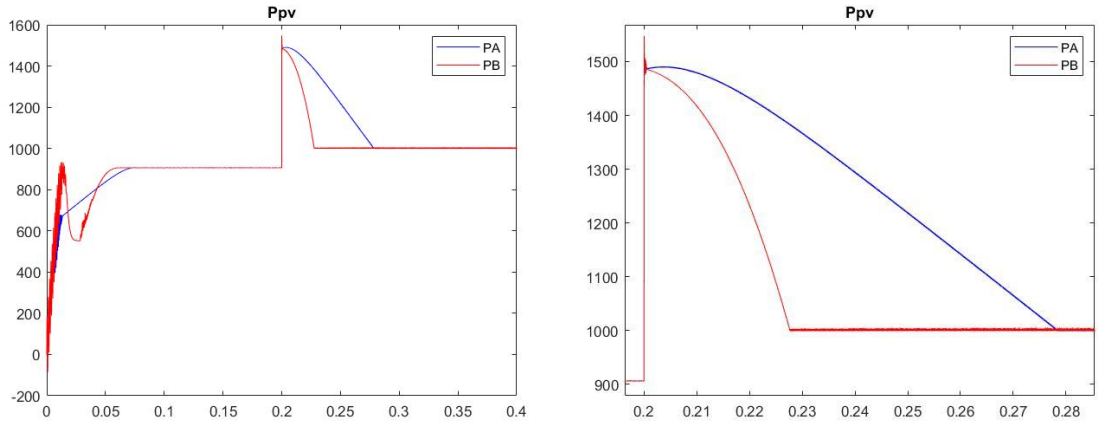

Figure 5.20 Irradiance Case 4: RPPT response

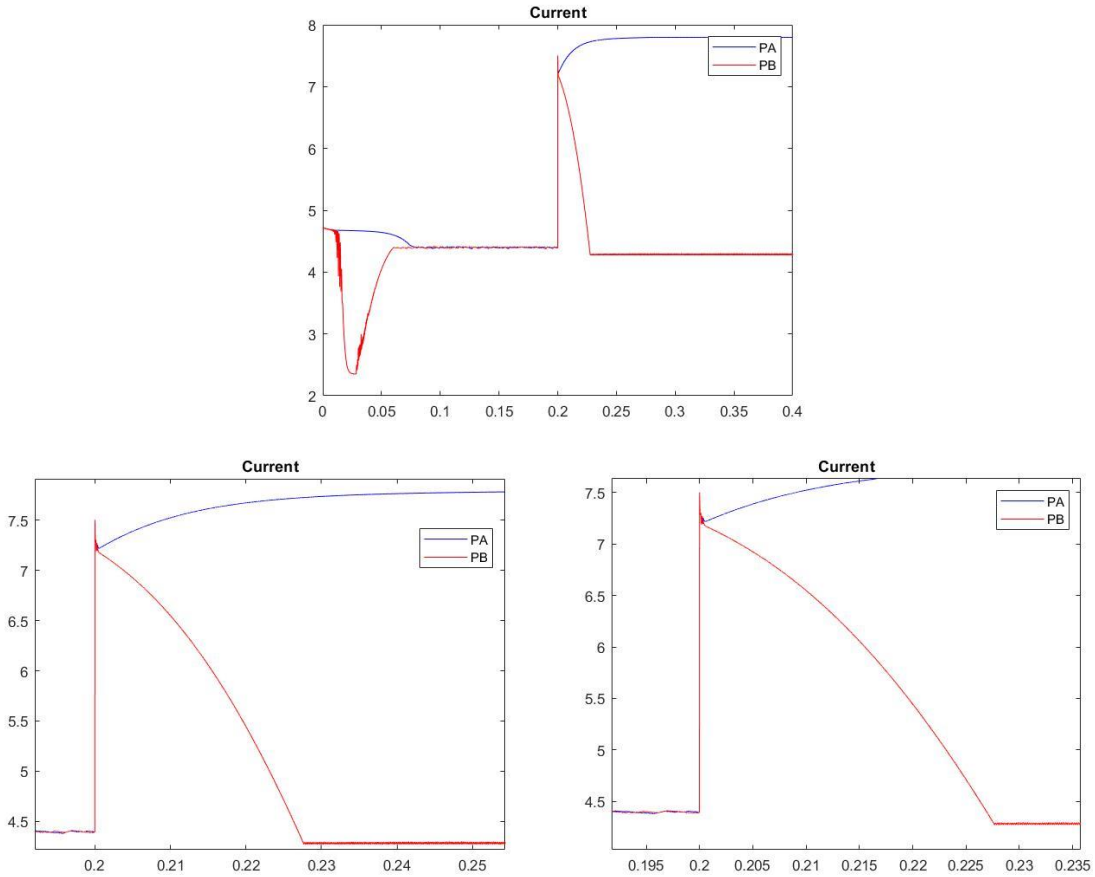

Figure 5.21 Irradiance Case 4: Current

Figure 5.21 shows the current response during the simulation. For the right-side, the current variation is very little, from 4.39A to 4.28A on average. The peak of power is occurring by the current and is 7.49A. Oscillations are seen bigger than for the left-side. For the left-side, the current is helped by the increased of the irradiance and can therefore converge slowly to the stable point. The current goes from 4.39A to 7.79A.

Figure 5.22 shows the voltage reaction during the simulation. For the left-side, the voltage varies form 206V to 128V. For the right-side, the voltage varies from 206V to 233V on average.

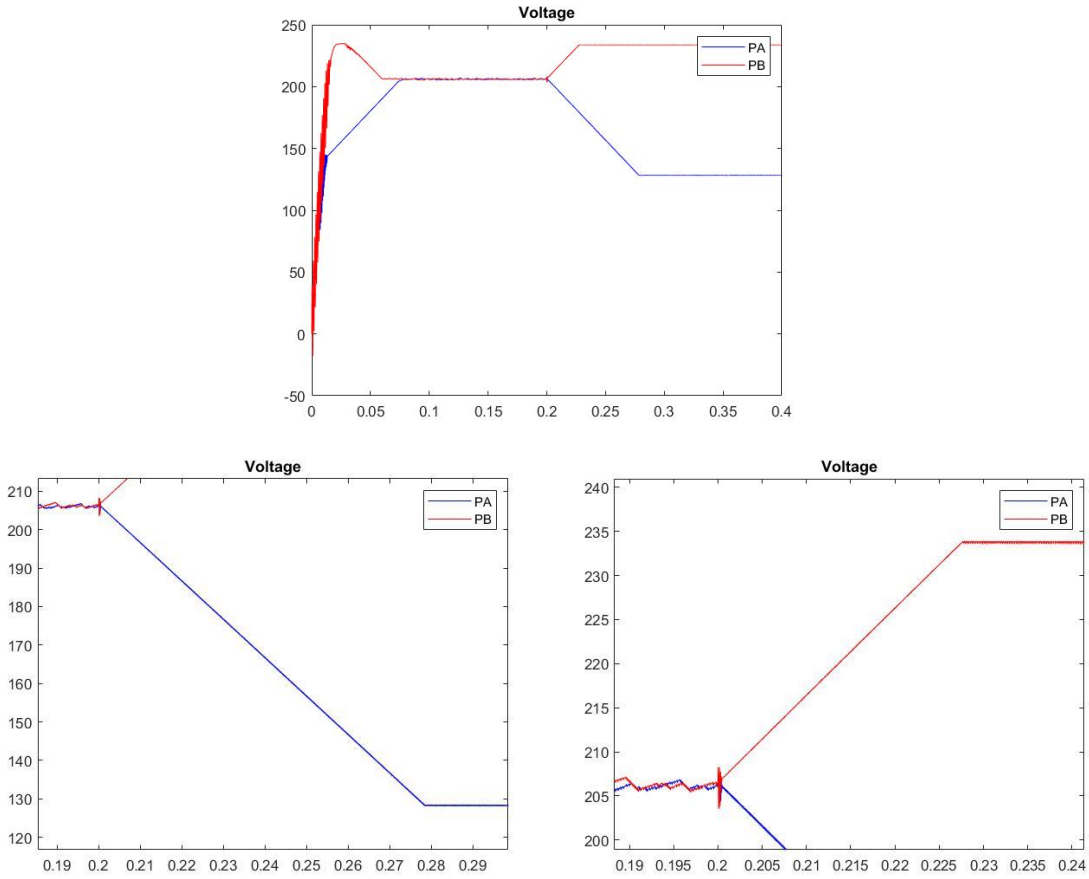

Figure 5.22 Irradiance Case 4: Voltage

Table 5.5Table 5.2 sumarizes the main characteristics.

Table 5.5 Resume of the Irradiation Case 4

	Left-side	**Right-side**
Peak (W)	1489	1547
Time (ms)	79	28
ΔI(A)	3.4	0.11
ΔV (V)	78	27

5.3 Case with Variation of the required load power

Now, the irradiance is kept at 1000W/m² and the temperature at 25°C.

5.3.1 Case 1: Step-down response

Figure 5.23 shows the maximum power available with the load power variation. During 0.2s, the load power is kept at 2000W and then goes to 1000W. This drives the system to jump from MPPT mode to the RPPT mode.

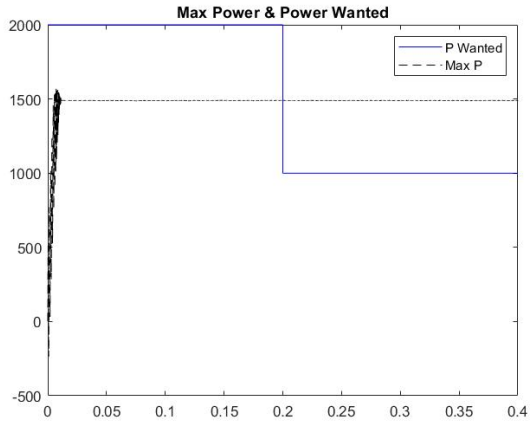

Figure 5.23 Power load Case 1: Maximum Power available

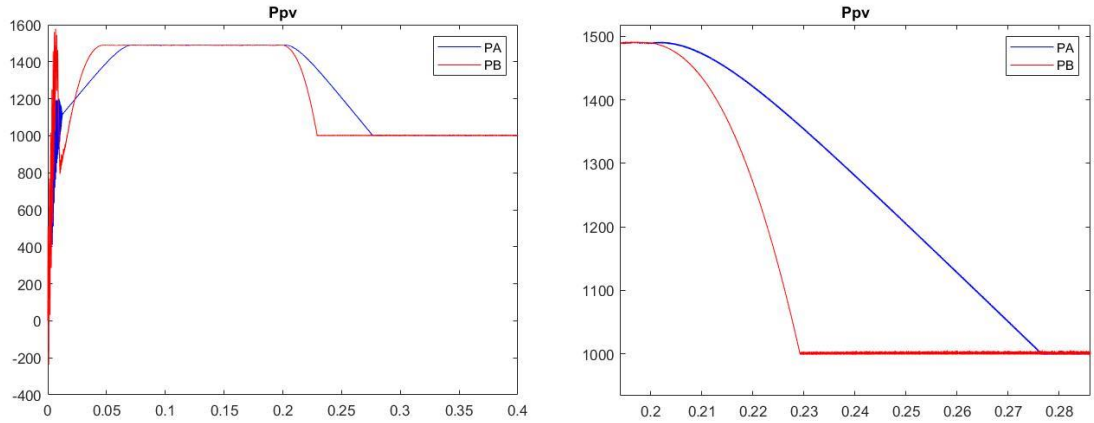

Figure 5.24 Power load Case 1: RPPT response

Figure 5.24 shows that the MPP is reached and then the power converges to 1000W. For the left-side the time to converge takes 78ms while the right-side takes 29ms. The shape of the PV-Curve can be seen on the figure.

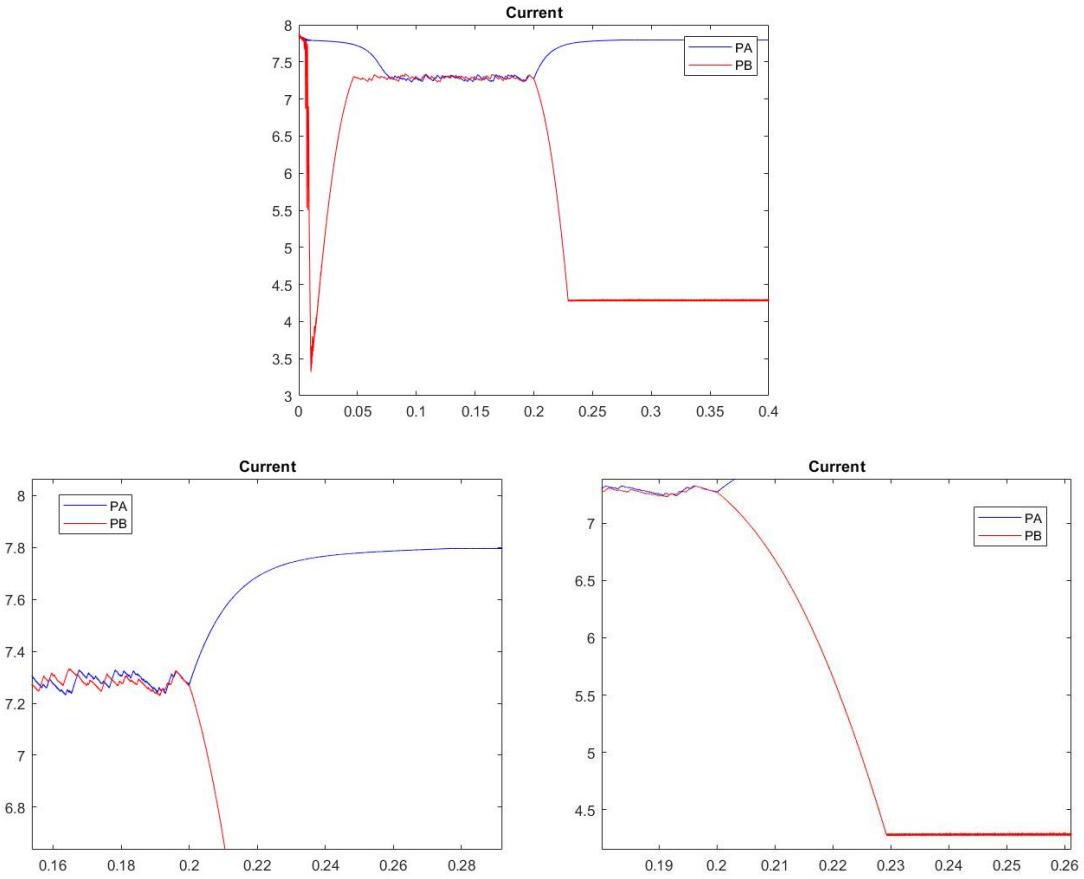

Figure 5.25 Power load Case 1: Current

Figure 5.25 shows the current reaction during the simulation. For the left-side the current goes from 7.28A to 7.79A while the right-side goes from 7.28A to 4.29A. During the MPPT period, oscillations can be noticed.

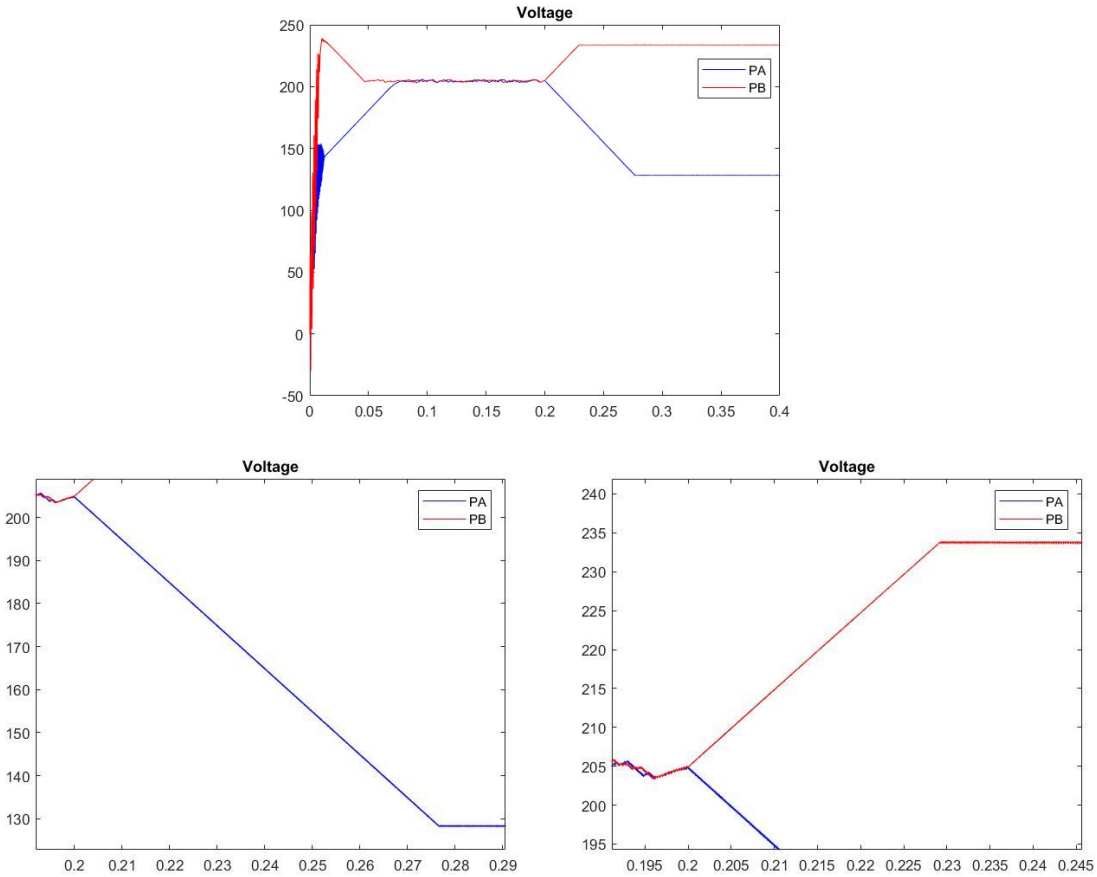

Figure 5.26 Power load Case 1: Voltage

Figure 5.26 shows the voltage reaction during the simulation. For the right-side the voltage goes from 204V to 233V while the left-side goes from 204V to 128V.

5.3.2 Case 2: Step-up response

Figure 5.27 shows the maximum power available with the load power variation. During 0.2s, the load power is kept at 1000W and then goes to 2000W. This drives the system to jump from RPPT mode to the MPPT mode.

Figure 5.27 Power load Case 2: Maximum Power available

Figure 5.28 shows that the power when 1000W is reached and then the power converges to the MPP. For the left-side the time to converge takes 71ms while the for the right-side it takes 23ms. The shape of the PV-Curve can be seen on the figure.

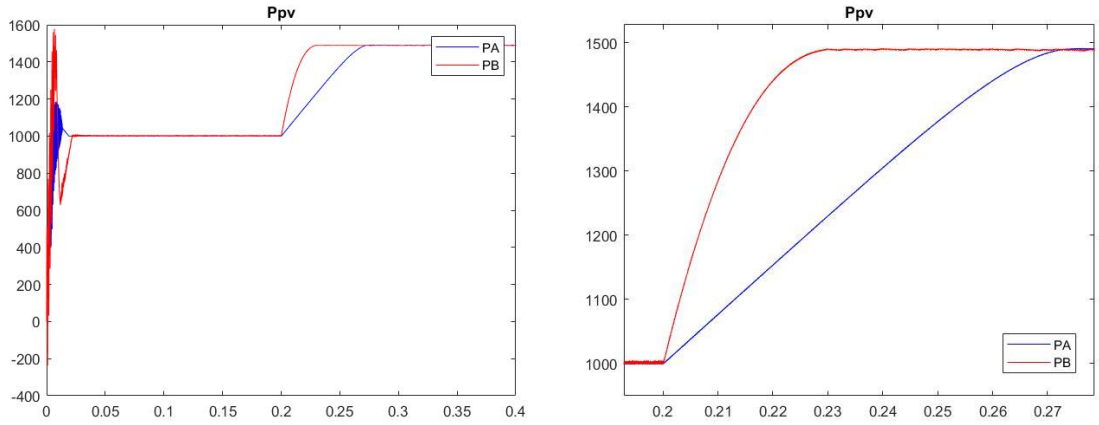

Figure 5.28 Power load Case 2: RPPT response

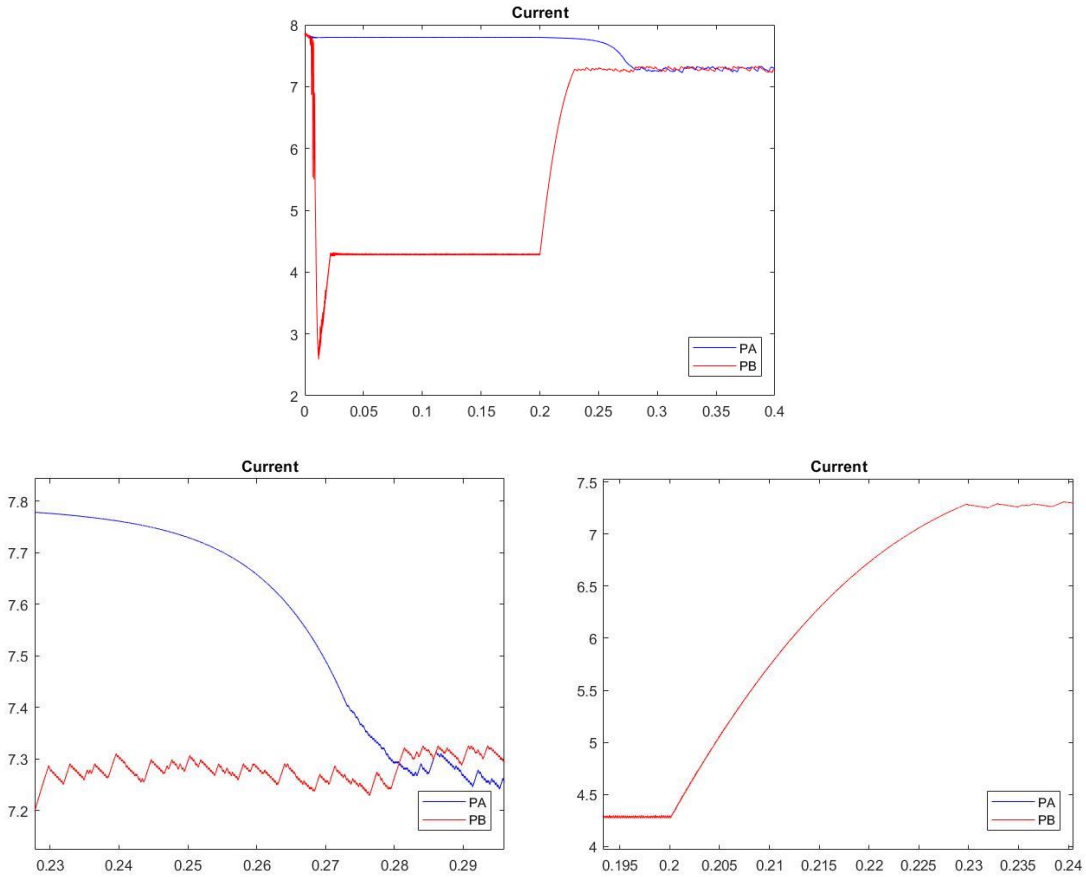

Figure 5.29 Power load Case 2: Current

Figure 5.29 shows the current response during the simulation. For the left-side the current goes from 7.79A to 7.28A while for the right-side it goes from 4.29A to 7.28A. During the MPPT period, oscillations can be noticed.

Figure 5.30 shows the voltage response during the simulation. For the right-side the voltage goes from 233V to 204V while for the left-side goes from 128V to 204V. During the convergence, the response is similar to a ramp.

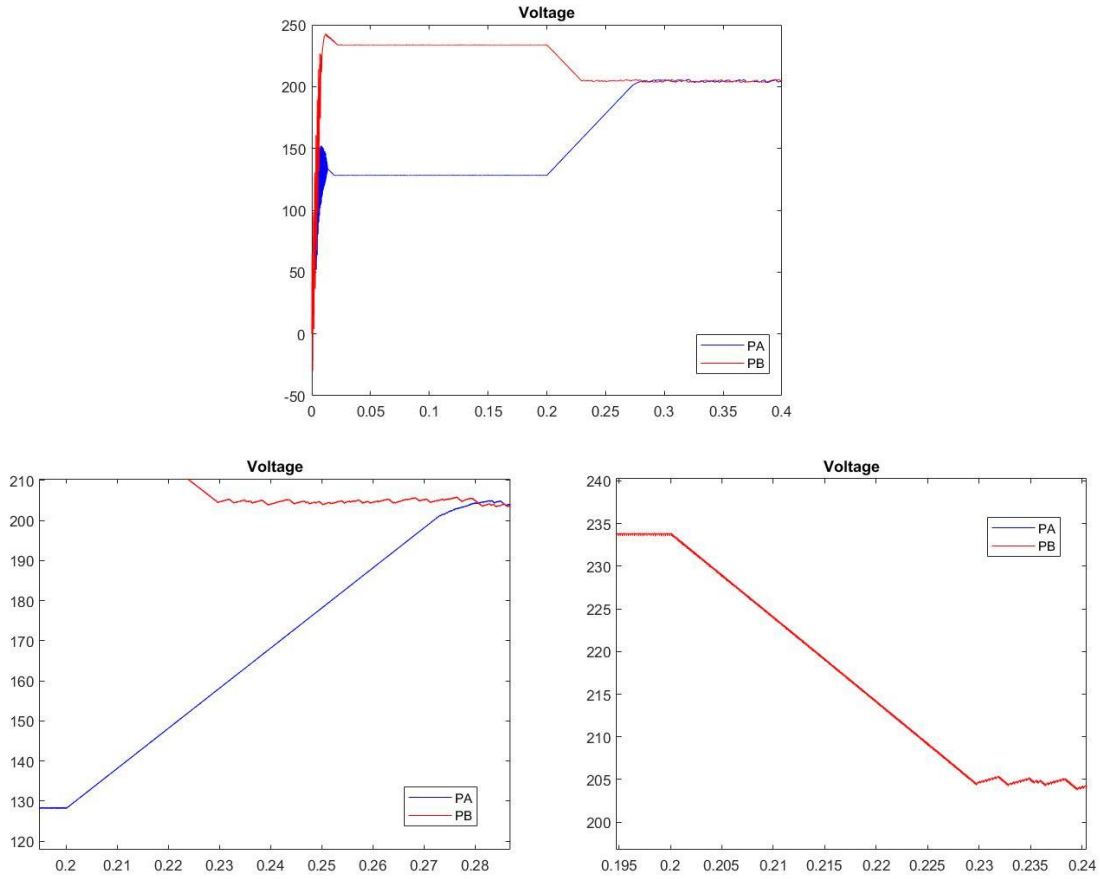

Figure 5.30 Power load Case 2: Voltage

5.3.3 Case 3: Two step-down responses

Figure 5.31 shows the maximum power available with the load power variation. During 0.15s, the load power is kept at 2000W and then goes to 1000W during 0.1s. At 0.25s, the load power goes to 500W. This drives the system to jump from MPPT mode to the RPPT mode.

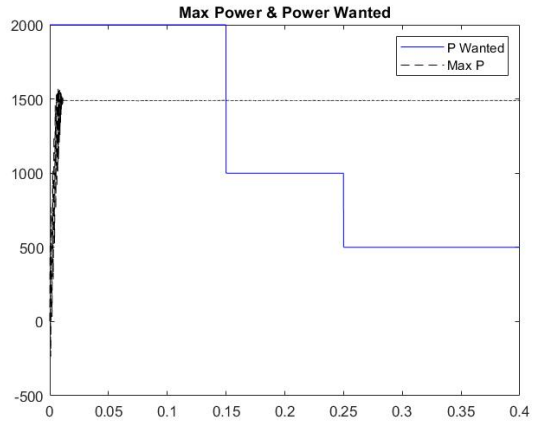

Figure 5.31 Power load Case 3: Maximum Power available

Figure 5.32 shows the RPP response. It goes first to the MPP, and then stabilize to 1000W and finally to 500W. The main problem on this figure is for the right-side, the RPPT has lost the tracking. It is not able to reach the 500W power requested and converges to 592W. For the left-side, the convergence is reached.

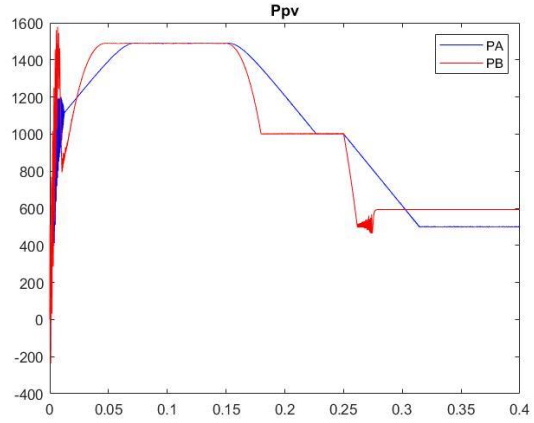

Figure 5.32 Power load Case 3: RPPT response

Figure 5.33 shows the current and the voltage during the simulation. For the left-side, the current variation is very small, while the voltage drops is significant. At each step, the point is reached after 82ms. For the right-side, the point is reached faster, but when 500W is asked by the load power, the tracking is lost. Thus, there exists a limit for the right-side, where the tracking become inefficient.

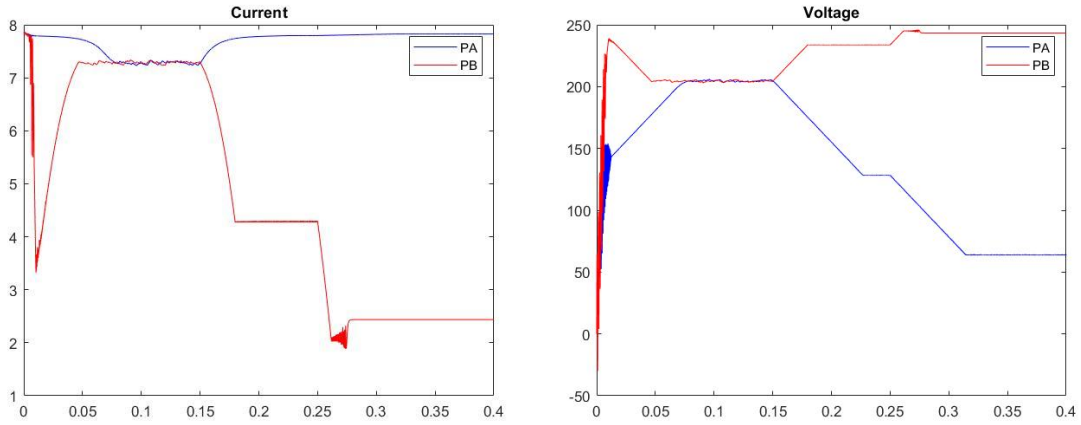

Figure 5.33 Power load Case 3: Current and Voltage

5.3.4 Case 4: Two step-up responses

Figure 5.34 shows the maximum power available with the load power variation. During 0.15s, the load power is kept at 500W and then goes to 1000W during 0.1s. At 0.25s, the load power goes to 1000W. This drives the system to jump from MPPT mode to the RPPT mode.

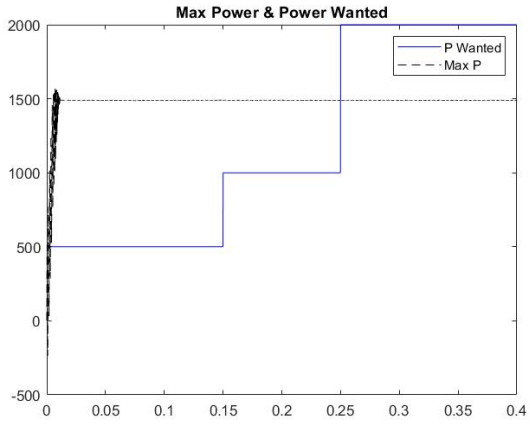

Figure 5.34 Power load Case 4: Maximum Power available

Figure 5.35 shows the simulation for the right-side and the left-side. For the left-side, the tracking is functioning, while for the right-side, the tracking is lost from the beginning.

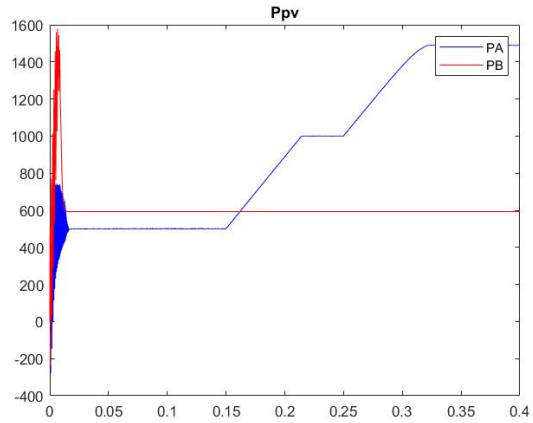

Figure 5.35 Power load Case 4: RPPT response

Figure 5.36 shows the current and the voltage during the simulation. The right-side cannot reach the voltage requested.

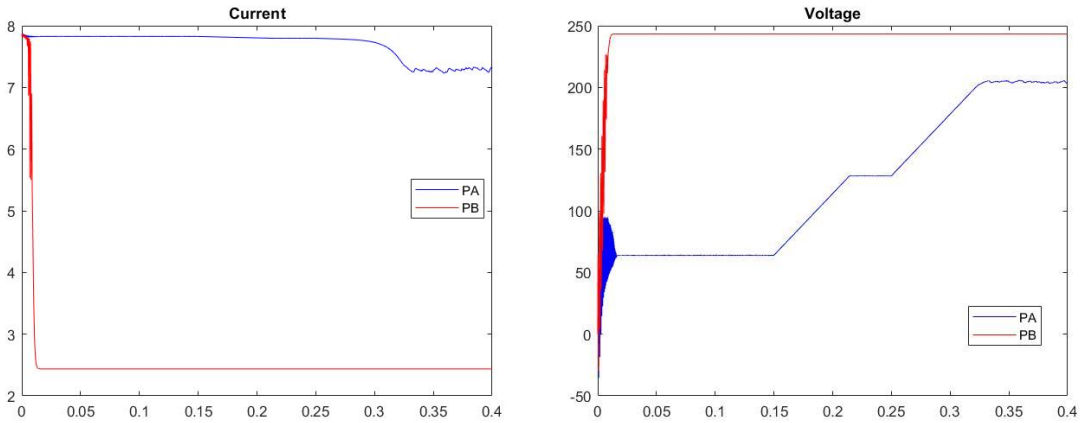

Figure 5.36 Power load Case 4: Current and Voltage

Chapter 6
Conclusions

The purpose of this work was to present the validation of the best point to operate while using the Reduced Power Point Tracking algorithm which represents an alternative to the Maximum Power Point Tracking. The theory of the RPPT has been deeply developed for the two candidates, the left-side RPP (point PA) and the right-side RPP (point PB), and simulations have confirmed the results expected by the theory.

The point PA presents a slower time of convergence. This gives the time for the system a strong stability. With this stability, the power is able to converge with a very small static error.
The point PB presents a faster time of convergence. Due to this short time, oscillations are are considerable which impacts the stability. If any perturbation occurs, the system can collapse and lose the tracking. The oscillations are mainly due to the current response because the range of application is narrower, and a small variation of the voltage gives a higher current range.
Comparing with all the result obtained during this study, the RPPT algorithm on the left-side presents better advantages than on the right-side. It is important to remind that many parameters are determining this result.

Now the point PA has been defined as the best operating point for the RPPT algorithm, the voltage range for the algorithm can be reduced to $[0; 1.1 \cdot V_{MPP}]$. The RPPT algorithm using P&O as a base can be compared to other algorithms so as to define which one is the best in RPPT.
This thesis objective can be pushed throught with further simulations such as the study of this model's stability for 24h time. and the next work would be the analysis of the stability of the RPPT algorithm over a day period, then the analysis of the PV system coupled with a storage system and finally the analysis of the energy production curtailed over a day period. In order to get closer and closer to full contrability of the photovoltaic energy production to reach a change in the paradigm of global renewable energy production.

Bibliography

[1] European Commission, “REPORT FROM THE COMMISSION TO THE EUROPEAN PARLIAMENT, THE COUNCIL, THE EUROPEAN ECONOMIC AND SOCIAL COMMITTEE AND THE COMMITTEE OF THE REGIONS,” 2019.

[2] A. J.-W. IEA PVPS,Becquerel Institute, RTS Corporation, “Snapshot of Global PV Markets,” 2019.

[3] European Commission, “PHOTOVOLTAIC BAROMETER,” no. April 2019, 2018.

[4] P. A. Lynn, *Electricity from Sunlight: An Introduction to Photovoltaics*. John Wiley & Sons, 2010.

[5] F. Foiadelli, “Photovoltaic System,” 2016.

[6] S. Kouro, B. Wu, H. Abu-rub, and F. Blaabjerg, “Photovoltaic Energy Conversion Systems,” 2014.

[7] B. Nusillard and M. Olmi, “Development of Generalized Photovoltaic Model Using MATLAB/SIMULINK,” in *Entomologist’s Gazette*, 2008, vol. 59, no. 3, pp. 199–208.

[8] G. M. Masters, *Renewable and efficient electric power systems*, vol. 42, no. 06. 2005.

[9] H. Machrafi, *Green Energy and Technology*. 2012.

[10] X. H. Nguyen and M. P. Nguyen, “Mathematical modeling of photovoltaic cell/module/arrays with tags in Matlab/Simulink,” *Environ. Syst. Res.*, vol. 4, no. 1, 2015.

[11] C. Sharma and A. Jain, “Solar Panel Mathematical Modeling Using Simulink,” *Int. J. Eng. Res. Appl.*, vol. 4, no. 5, pp. 67–72, 2014.

[12] J. Ahmed and Z. Salam, “A Modified P and O Maximum Power Point Tracking Method with Reduced Steady-State Oscillation and Improved Tracking Efficiency,” *IEEE Trans. Sustain. Energy*, vol. 7, no. 4, pp. 1506–1515, 2016.

[13] T. Esram, J. W. Kimball, P. T. Krein, P. L. Chapman, and P. Midya, “Dynamic maximum power point tracking of photovoltaic arrays using ripple correlation control,” *IEEE Trans. Power Electron.*, vol. 21, no. 5, pp. 1282–1290, 2006.

[14] B. Yu, G. Yu, and Y. Kim, “Design and experimental results of improved dynamic MPPT performance by EN50530,” *INTELEC, Int. Telecommun. Energy Conf.*, no. 2009t1 00200094, 2011.

[15] T. Esram and P. L. Chapman, “Comparison of photovoltaic array maximum power point tracking techniques,” *IEEE Trans. Energy Convers.*, vol. 22, no. 2, pp. 439–449, 2007.

[16] R. Faranda, S. Leva, and V. Maugeri, “MPPT techniques for PV systems: Energetic and cost comparison,” *IEEE Power Energy Soc. 2008 Gen. Meet. Convers. Deliv. Electr. Energy 21st Century, PES*, pp. 1–6, 2008.

[17] A. DOLARA, R. FARANDA, and S. LEVA, “Energy Comparison of Seven MPPT Techniques for PV Systems,” *J. Electromagn. Anal. Appl.*, vol. 01, no. 03, pp. 152–162, 2009.

[18] M. Berrera, A. Dolara, R. Faranda, and S. Leva, “Experimental test of seven widely-adopted MPPT algorithms,” *2009 IEEE Bucharest PowerTech Innov. Ideas Towar. Electr. Grid Futur.*, pp. 1–8, 2009.
[19] E. Kabalci, “Maximum power point tracking (MPPT) algorithms for photovoltaic systems,” *Lect. Notes Energy*, vol. 37, pp. 205–234, 2017.
[20] G. Remy, O. Bethoux, C. Marchand, and H. Dogan, “Review of MPPT Techniques for Photovoltaic Systems,” 2009.
[21] M. Liserre and P. R. R. Teodorescu, *Grid Converters for Photovoltaic and Wind Power Systems Chapter 10 Control of Grid Converters under Grid F lt Faults*. 2011.
[22] B. Zhao, C. Wang, and X. Zhang, *Grid-Integrated and Standalone Photovoltaic Distributed Generation Systems*. 2017.
[23] R. Algerienne, D. Et, E. Scientifique, F. D. E. Technologie, and D. D. E. G. Electrique, “Commande par mode de glissement des convertisseurs Buck et Boost intégrés dans un système photovoltaïque,” 2016.
[24] H. Yao, “MODELING AND DESIGN OF A CURRENT MODE CONTROL BOOST CONVERTER,” 2012.
[25] Texas Instruments, “Practical Feedback Loop Analysis for Current-Mode Boost Converter,” *Appl. Report, SLVA636*, no. January, pp. 1–14, 2014.
[26] D. Imen, “COMMANDE DES SYSTEMES NON LINEAIRES PAR MODE GLISSANT D’ORDRE SUPERIEUR,” 2013.
[27] M. Senesky, G. Eirea, and T. J. Koo, “Hybrid modelling and control of power electronics,” *Lect. Notes Comput. Sci. (including Subser. Lect. Notes Artif. Intell. Lect. Notes Bioinformatics)*, vol. 2623, pp. 450–465, 2003.